



1 **Source Apportionment of Fine Aerosol at an Urban Site of Beijing**  
2 **using a Chemical Mass Balance Model**

3  
4 **Jingsha Xu<sup>1</sup>, Di Liu<sup>1,2</sup>, Xuefang Wu<sup>1,3</sup>, Tuan V. Vu<sup>1,4</sup>, Yanli Zhang<sup>5</sup>, Pingqing Fu<sup>6</sup>, Yele Sun<sup>7</sup>, Weiqi**  
5 **Xu<sup>7</sup>, Bo Zheng<sup>8,9</sup>, Roy M. Harrison<sup>1,\*</sup>, Zongbo Shi<sup>1,\*</sup>**

- 6  
7 1 School of Geography Earth and Environmental Science, University of Birmingham, Birmingham, B15 2TT, UK  
8 2 Now at: Institute of Atmospheric Physics, Chinese Academy of Sciences, Beijing, 100029, China  
9 3 School of Geology and Mineral Resources, China University of Geosciences Xueyuan Road 29, Beijing, 100083, China  
10 4 Now at: Faculty of Life Sciences & Medicine, King's College London, London, WC2R 2LS, UK  
11 5 Guangzhou Institute of Geochemistry, Chinese Academy of Sciences, Guangzhou, 510640, China  
12 6 Institute of Surface-Earth System Science, Tianjin University, Tianjin, 300072, China  
13 7 State Key Laboratory of Atmospheric Boundary Layer Physics and Atmospheric Chemistry, Institute of Atmospheric Physics,  
14 Chinese Academy of Sciences, Beijing, 100029, China  
15 8 State Key Joint Laboratory of Environment Simulation and Pollution Control, School of Environment, Tsinghua University,  
16 Beijing, 100084, China  
17 9 Now at: Laboratoire des Sciences du Climat et de l'Environnement, CEA-CNRS-UVSQ, UMR8212, Gif-sur-Yvette, France

18  
19 \*Correspondence: Zongbo Shi (Z.Shi@bham.ac.uk) and Roy Harrison (r.m.harrison@bham.ac.uk)

20 **Abstract**

21  
22  
23 Fine particles were sampled from 9<sup>th</sup> November to 11<sup>th</sup> December 2016 and 22<sup>nd</sup> May  
24 to 24<sup>th</sup> June 2017 as part of the Atmospheric Pollution and Human Health in a Chinese  
25 megacity (APHH-China) field campaigns in urban Beijing, China. Inorganic ions, trace  
26 elements, OC, EC, and organic compounds including biomarkers, hopanes, PAHs, n-  
27 alkanes and fatty acids, were determined for source apportionment in this study.  
28 Carbonaceous components contributed on average 47.2% and 35.2% of total  
29 reconstructed PM<sub>2.5</sub> during the winter and summer campaigns, respectively. Secondary  
30 inorganic ions (sulfate, nitrate, ammonium; SNA) accounted for 35.0% and 45.2% of  
31 total PM<sub>2.5</sub> in winter and summer. Other components including inorganic ions (K<sup>+</sup>, Na<sup>+</sup>,  
32 Cl<sup>-</sup>), geological minerals, and trace metals only contributed 13.2% and 12.4% of PM<sub>2.5</sub>  
33 during the winter and summer campaigns. Fine OC was explained by seven primary  
34 sources (industrial/residential coal burning, biomass burning, gasoline/diesel vehicles,  
35 cooking and vegetative detritus) based on a chemical mass balance (CMB) receptor  
36 model. It explained an average of 75.7% and 56.1% of fine OC in winter and summer,  
37 respectively. Other (unexplained) OC was compared with the secondary OC (SOC)  
38 estimated by the EC-tracer method, with correlation coefficients (R<sup>2</sup>) of 0.58 and 0.73,  
39 and slopes of 1.16 and 0.80 in winter and summer, respectively. This suggests that the  
40 unexplained OC by CMB was mostly associated with SOC. PM<sub>2.5</sub> apportioned by CMB  
41 showed that the SNA and secondary organic matter were the highest two contributors  
42 to PM<sub>2.5</sub>. After these, coal combustion and biomass burning were also significant  
43 sources of PM<sub>2.5</sub> in winter. The CMB results were also compared with results from  
44 Positive Matrix Factorization (PMF) analysis of co-located Aerosol Mass Spectrometer  
45 (AMS) data. The CMB was found to resolve more primary OA sources than AMS-PMF  
46 but the latter apportioned more secondary OA sources. The AMS-PMF results for major  
47 components, such as coal combustion OC and oxidized OC correlated well with the  
48 results from CMB. However, discrepancies and poor agreements were found for other  
49 OC sources, such as biomass burning and cooking, some of which were not identified  
50 in AMS-PMF factors.



51

52 **Keywords:** PM<sub>2.5</sub>, Beijing, mass closure, CMB, AMS-PMF, source apportionment



## 53 1 Introduction

54 Beijing is the capital of China and a hotspot of particulate matter pollution. It has been  
55 experiencing severe PM<sub>2.5</sub> (particulate matter with an aerodynamic diameter of  
56  $\leq 2.5\mu\text{m}$ ) pollution in recent decades, as a result of rapid urbanization and  
57 industrialization, and increasing energy consumption (Wang et al., 2009). High PM<sub>2.5</sub>  
58 pollution from Beijing could have significant impact on human health (Song et al.,  
59 2006a; Li et al., 2013). A case study in Beijing revealed that a  $10\ \mu\text{g m}^{-3}$  increase of  
60 ambient PM<sub>2.5</sub> concentration will correspondingly increase 0.78%, 0.85% and 0.75%  
61 of the daily mortality of the circulatory diseases, cardiovascular diseases and  
62 cerebrovascular diseases, respectively (Dong et al., 2013). Furthermore, PM<sub>2.5</sub> causes  
63 visibility deterioration in Beijing. A better understanding of the sources of PM<sub>2.5</sub> in  
64 Beijing is essential to provide scientific evidence to control the PM<sub>2.5</sub> pollution.

65 Many studies have identified the possible sources of fine particulate matter in Beijing  
66 using various methods (Zheng et al., 2005; Song et al., 2006a; Song et al., 2006b; Li et  
67 al., 2015; Zhang et al., 2013; Yu and Wang, 2013). Song et al. (2006a) applied  
68 two eigenvector models, principal component analysis/absolute principal component  
69 scores (PCA/APCS) and UNMIX to study the sources of PM<sub>2.5</sub> in Beijing. Some studies  
70 used elemental tracers to do source apportionment of PM<sub>2.5</sub> by applying positive matrix  
71 factorization (PMF) (Song et al., 2006b; Li et al., 2015; Zhang et al., 2013; Yu and  
72 Wang, 2013). This approach has some underlying issues: firstly, PMF requires a  
73 relatively large sample size; and a “best” solution of achieved factors is subjective  
74 (Ulbrich et al., 2009); secondly, many important PM<sub>2.5</sub> emission sources do not have a  
75 unique elemental composition. Hence, an elemental tracer-based method cannot  
76 distinguish sources such as cooking or vehicle exhaust, as they emit mainly  
77 carbonaceous compounds (Wang et al., 2009). Generally, organic matter (OM) is  
78 comprised of primary organic matter (POM) and secondary organic matter (SOM).  
79 POM is directly emitted and SOM is formed through chemical oxidation of volatile  
80 organic compounds (VOCs) (Yang et al., 2016). OM was the largest contributor to  
81 PM<sub>2.5</sub> mass, which accounted for 30%-60% of PM<sub>2.5</sub> (Song et al., 2007; He et al., 2001;  
82 Huang et al., 2014), and can contribute up to 90% of submicron PM mass (Zhou et al.,  
83 2018). Furthermore, many organic tracers are more specific to particular sources,  
84 making them more suitable to identify and quantify different source contributions to  
85 carbonaceous aerosols and PM<sub>2.5</sub>.

86 A few studies have also applied a Chemical Mass balance (CMB) model for source  
87 apportionment of PM in Beijing. For example, Zheng et al. (2005) investigated sources  
88 of PM<sub>2.5</sub> in Beijing, but the source profiles they used were mainly derived in the United  
89 States, which were less representative of the local sources. Liu et al. (2016) and Guo et  
90 al. (2013) apportioned the sources of PM<sub>2.5</sub> in a typical haze episode in winter 2013 in  
91 Beijing during the Olympic Games period in summer 2008, respectively. Wang et al.  
92 (2009) apportioned the sources of PM<sub>2.5</sub> in both winter and summer. A major challenge  
93 of the CMB model is that it cannot quantify the contributions of secondary organic  
94 aerosol and unknown sources, which are often lumped as “unexplained OC”.

95 In this study, PM<sub>2.5</sub> samples were collected in an urban site of Beijing during winter  
96 and summer 2016-2017. OC, EC, PAHs, alkanes, hopanes, fatty acids and  
97 monosaccharide anhydrides were determined. To ensure that the source profiles used in

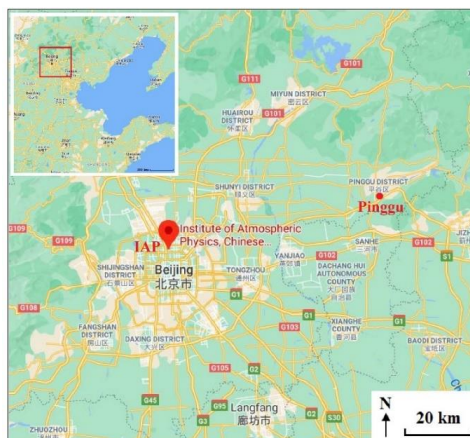


98 the CMB model are representative, we mainly selected those studies which had been  
99 based in China: straw burning (Zhang et al., 2007b), wood burning (Wang et al., 2009),  
100 gasoline and diesel vehicles (Cai et al., 2017), industrial and residential coal combustion  
101 (Zhang et al., 2008), and cooking (Zhao et al., 2015). Source contributions of organic  
102 carbon were examined and quantified applying the CMB model based on the source  
103 profiles mentioned above. The results of this study are discussed and compared with  
104 the results from Aerosol Mass Spectrometer-PMF analysis (AMS-PMF) (Ulbrich et al.,  
105 2009; Elser et al., 2016) to improve our understanding of different sources of PM<sub>2.5</sub>,  
106 especially for secondary organic aerosols.

## 107 2 Methodology

### 108 2.1 Aerosol sampling

109 PM<sub>2.5</sub> was collected at an urban sampling site (116.39E, 39.98N) - the Institute of  
110 Atmospheric Physics (IAP) of the Chinese Academy of Sciences in Beijing, China from  
111 9<sup>th</sup> November to 11<sup>th</sup> December 2016 and 22<sup>nd</sup> May to 24<sup>th</sup> June 2017, as part of the  
112 Atmospheric Pollution and Human Health in a Chinese megacity (APHH-China) field  
113 campaigns (Shi et al., 2019). The sampling site (Fig. 1) is located in the middle between  
114 the North 3<sup>rd</sup> Ring Road and North 4<sup>th</sup> Ring Road and approximately 200 m from a  
115 major highway. Hence, it is subject to many local sources, such as traffic, cooking, etc.  
116 The location of a rural site in Beijing - Pinggu during the APHH-China campaigns is  
117 also shown in Fig. 1. Other information regarding the sampling site is described  
118 elsewhere (Shi et al., 2019).



119  
120 **Figure 1.** Locations of the sampling sites in Beijing (IAP - urban site: Institute of Atmospheric Physics  
121 of the Chinese Academy of Sciences; Pinggu - rural site) (source: © Google Maps).

122 PM<sub>2.5</sub> samples were collected on pre-baked (450°C for 6h) large quartz filters  
123 (Pallflex, 8×10 inch) by Hi-Vol air sampler (Tisch, USA) at a flow rate of 1.1 m<sup>3</sup> min<sup>-1</sup>.  
124 A Medium-Vol air sampler (Thermo Scientific Partisol 2025i) was also deployed at  
125 the same location to collect PM<sub>2.5</sub> samples simultaneously on 47 mm PTFE filters at a  
126 flow rate of 15.0 L min<sup>-1</sup>. Field blanks were also collected with the pump turned off  
127 during the sampling campaign. Before and after sampling, all filters were put in a



128 balance room and equilibrated at a constant temperature and relative humidity (RH) for  
129 24h prior to any gravimetric measurements, which were 22°C and 30% RH for summer  
130 samples, 21°C and 33% RH for winter samples. PM<sub>2.5</sub> mass was determined through  
131 the weighing of PTFE filters using a microbalance (Sartorius model MC5, precision: 1  
132 µg). After that, filters were wrapped separately with aluminum foil and stored at under  
133 -20°C in darkness until analysis. The large quartz filters were analyzed for OC, EC,  
134 organic compounds and ion species, while small PTFE filters were used for the  
135 determination of PM<sub>2.5</sub> mass and metals. Online PM<sub>2.5</sub> were determined by the TEOM  
136 FDMS 1405-DF instrument at IAP with filter equilibrating and weighing conditions  
137 comparable with the Federal Reference Method (RH: 30-40%; temperature; 20-23°C).

## 138 2.2 Chemical Analysis

### 139 2.2.1 OC and EC

140 A 1.5 cm<sup>2</sup> punch from each large quartz filter sample was taken for organic carbon (OC)  
141 and elemental carbon (EC) measurements by a thermal/optical carbon analyzer (model  
142 RT-4, Sunset Laboratory Inc., USA) based on the EUSAAR2 (European Supersites for  
143 Atmospheric Aerosol Research) transmittance protocol. The uncertainties from  
144 duplicate analyses of filters were <10%. Replicate analyses were conducted once every  
145 ten samples. All sample results were corrected by the values obtained from field blanks,  
146 which were 0.40 and 0.01 µg m<sup>-3</sup> for OC and EC, respectively. Details of the OC/EC  
147 measurement method can be found elsewhere (Paraskevopoulou et al., 2014). The  
148 instrumental limits of detection of OC and EC in this study were estimated to be 0.03  
149 and 0.05 µg m<sup>-3</sup>, respectively.

### 151 2.2.2 Organic compounds

152 Organic tracers, including 11 n-alkanes (C<sub>24</sub>-C<sub>34</sub>), 2 hopanes (17a (H) -22, 29, 30-  
153 Trisnorhopane, 17b (H), 21a (H) -Norhopane), 17 PAHs (retene, phenanthrene,  
154 anthracene, fluoranthene, pyrene, benz(a)anthracene, chrysene, benzo(b)fluoranthene,  
155 benzo(k)fluoranthene, benzo(e)pyrene, benzo(a)pyrene, perylene, Indeno(1,2,3-  
156 cd)pyrene, dibenz(a,h)anthracene, benzo(ghi)perylene, coronene, picene), 3  
157 anhydrosugars (levoglucosan, mannosan, galactosan), 2 fatty acids (palmitic acid,  
158 stearic acid) and cholesterol in the PM<sub>2.5</sub> samples were determined in this study. A  
159 portion of the filters were extracted 3 times with dichloromethane/methanol (HPLC  
160 grade, v/v: 2:1) under ultrasonication for 10 minutes. The extracts were then filtered  
161 and concentrated using a rotary evaporator under vacuum, and blown down to dryness  
162 with pure nitrogen gas. 50 µL of N,O-bis-(trimethylsilyl)trifluoroacetamide (BSTFA)  
163 with 1% trimethylsilyl chloride and 10 µL of pyridine were then added to the extracts,  
164 which were left reacting at 70 °C for 3 h to derivatize -COOH to TMS esters and -OH  
165 to TMS ethers. After cooling to room temperature, the derivatives were diluted with  
166 140 µL of internal standards (C<sub>13</sub> n-alkane, 1.43 ng µL<sup>-1</sup>) in n-hexane prior to GC-MS  
167 analysis. The final solutions were analyzed by a gas chromatography mass spectrometry  
168 system (GC/MS, Agilent 7890A GC plus 5975C mass-selective detector) fitted with a  
169 DB-5MS column (30 m × 0.25 mm × 0.25 µm). The GC temperature program and MS  
170 detection details were reported in Li et al. (2018). Individual compounds were identified  
171 through the comparison of mass spectra with those of authentic standards or literature  
172 data (Fu et al., 2016). Recoveries for these compounds were in a range of 70-100%,



173 which were obtained by spiking standards to pre-baked blank quartz filters followed by  
174 the same extraction and derivatization procedures. Field blank filters were analyzed the  
175 same way as samples for quality assurance, but no target compounds were detected.

### 176 **2.2.3 Inorganic components**

177 Major inorganic ions including  $\text{Na}^+$ ,  $\text{K}^+$ ,  $\text{NH}_4^+$ ,  $\text{Cl}^-$ ,  $\text{NO}_3^-$  and  $\text{SO}_4^{2-}$  were determined by  
178 using an ion chromatograph (IC, Dionex, Sunnyvale, CA, USA), the detection limits  
179 (DLs) of them were 0.032, 0.010, 0.011, 0.076, 0.138, 0.240 and 0.142  $\mu\text{g m}^{-3}$   
180 respectively. The analytical uncertainty was less than 5% for all inorganic ions. An  
181 intercomparison study showed that our IC analysis of the above-mentioned ions agreed  
182 well with those of the other laboratories (Xu et al., 2020). Trace metal including Al  
183 (DLs in  $\mu\text{g m}^{-3}$ , 0.221), Si (0.040), Ca (0.034), Ti (0.003) and Fe (0.044) were  
184 determined by X-ray fluorescence spectrometer (XRF). Other elements including V, Cr,  
185 Co, Mn, Ni, Cu, Zn, As, Sr, Cd, Sb, Ba and Pb were analyzed by Inductively-coupled  
186 plasma-mass spectrometer (ICP-MS), the detection limits of them were 1.32, 0.25, 0.04,  
187 0.06, 2.05, 1.25, 1.22, 1.74, 0.02, 0.03, 0.11, 0.06 and 0.04  $\text{ng m}^{-3}$ , respectively. Mass  
188 concentrations of all inorganic ions and elements in this study were corrected for the  
189 field blank values, and the methods were quality assured with standard reference  
190 materials.

191

### 192 **2.3 Chemical Mass Closure (CMC) Method**

193 A Chemical Mass Closure analysis was carried out, which includes secondary inorganic  
194 ions (sulfate, nitrate, ammonium; SNA), sodium, potassium and chloride salts,  
195 geological minerals, trace elements, organic matter (OM), EC and bound water in  
196 reconstructed  $\text{PM}_{2.5}$ . Geological minerals were calculated applying the equation (Eq. 1)  
197 (Chow et al., 2015):

$$198 \text{ Geological minerals} = 2.2\text{Al} + 2.49\text{Si} + 1.63\text{Ca} + 1.94\text{Ti} + 2.42\text{Fe} \quad (1)$$

199 Trace elements were the sum of all analysed elements excluding Al, Si, Ca, Ti and  
200 Fe. The average OM/OC ratios of organic aerosols (OA) from AMS elemental analysis  
201 were applied to calculate OM, which were  $1.75 \pm 0.16$  and  $2.00 \pm 0.19$  in winter and  
202 summer, respectively. Based on the concentrations of inorganic ions and gas-phase  $\text{NH}_3$ ,  
203 particle bound water was calculated by ISORROPIA II model (available  
204 at <http://isorro피아.eas.gatech.edu>) in forward mode and thermodynamically metastable  
205 phase state (Fountoukis and Nenes, 2007). Two sets of calculations were done for online  
206 and offline data, differing at the temperature and relative humidity as specified above.

### 207 **2.4 Chemical Mass Balance (CMB) model**

208 A receptor model, namely the chemical mass balance model (US EPA CMB8.2), was  
209 applied in this study to apportion the sources of OC. It utilizes a linear least squares  
210 solution and both uncertainties in source profiles and ambient measurements were taken  
211 into consideration in this model. The essential criteria in this model were met to ensure  
212 reliable fitting results. For instance, in all samples,  $R^2$  were  $>0.80$  (mostly  $>0.9$ ),  $\text{Chi}^2$   
213 were  $<2$ , Tstat values were mostly greater than 2 except the source of vegetative  
214 detritus, and C/M ratios (ratio of calculated to measured concentration) for all fitting



215 species were in range of 0.8-1.2 in this study. The source profiles applied here were  
216 mostly from local studies in China to better represent the source characteristics,  
217 including straw burning (wheat, corn, rice straw burning) (Zhang et al., 2007b), wood  
218 burning (Wang et al., 2009), gasoline and diesel vehicles (including motorcycles, light-  
219 and heavy-duty gasoline and diesel vehicles) (Cai et al., 2017), industrial and residential  
220 coal combustion (including anthracite, sub-bituminite, bituminite, and brown coal)  
221 (Zhang et al., 2008), and cooking (Zhao et al., 2015), except vegetative detritus (Rogge  
222 et al., 1993; Wang et al., 2009). Fitting species should be stable during the transport  
223 from sources to receptor site and can represent the chemical characteristics of the  
224 sources (Wang et al., 2009). The selected fitting species were EC, levoglucosan,  
225 palmitic acid, stearic acid, fluoranthene, phenanthrene, retene, benz(a)anthracene,  
226 chrysene, benzo(b)fluoranthene, benzo(k)fluoranthene, benzo[ghi]perylene, picene,  
227 17a (H) -22, 29, 30-trisnorhopane, 17b (H), 21a (H) -norhopane and n-alkanes (C24-  
228 C33), the concentrations of which are provided in Table 1.

229

## 230 **2.5 Positive Matrix Factorization analysis of data obtained from Aerosol Mass** 231 **Spectrometer (AMS-PMF)**

232 An Aerodyne AMS with a PM<sub>1</sub> aerodynamic lens was deployed on the roof of the  
233 neighboring building- the Tower branch of IAP for real-time measurements of non-  
234 refractory (NR) chemical species from 15<sup>th</sup> November to 11<sup>th</sup> December 2016 and 22<sup>nd</sup>  
235 May to 24<sup>th</sup> June 2017. The detailed information of the sampling sites is given  
236 elsewhere (Xu et al., 2019b). The submicron particles were dried and sampled into the  
237 AMS at a flow of ~0.1 L min<sup>-1</sup>. NR-PM<sub>1</sub> can be quickly vaporized by the 600 °C  
238 tungsten vaporizer and then the NR-PM<sub>1</sub> species including organics, Cl<sup>-</sup>, NO<sub>3</sub><sup>-</sup>, SO<sub>4</sub><sup>2-</sup>  
239 and NH<sub>4</sub><sup>+</sup> were measured by AMS in mass sensitive V mode (Sun et al., 2020). Details  
240 of AMS data analysis, including the analysis of organic aerosol (OA) mass spectra can  
241 be found elsewhere (Xu et al., 2019b). While the source apportionment of fine OC in  
242 this study was conducted by using an offline chemical speciation dataset and source  
243 profiles, the source apportionment of organics in NR-PM<sub>1</sub> was carried out by applying  
244 PMF to the high-resolution mass spectra of OA. The procedures of the pretreatment of  
245 spectral data and error matrices can be found elsewhere (Ulbrich et al., 2009). The PMF  
246 analysis resulted in an optimal solution of 2 primary factors in summer: traffic-related  
247 hydrocarbon-like OA (HOA) and cooking OA (COA) and 3 secondary factors of  
248 oxygenated OA (OOA): OOA1, OOA2, OOA3. In winter, 3 primary factors were  
249 identified: coal combustion OA (CCOA), COA, biomass burning OA (BBOA), and 3  
250 secondary factors: oxidized primary OA (OPOA), less-oxidized OA (LOOOA), and  
251 more-oxidized OA (MOOOA). It is noted that the data were missing during the period  
252 09<sup>th</sup> - 14<sup>th</sup> November 2016 due to the malfunction of the AMS.

253

## 254 **3 Results and discussion**

### 255 **3.1 Characteristics of PM<sub>2.5</sub> and Carbonaceous Compounds**

256 Mean concentrations of PM<sub>2.5</sub>, OC, EC and organic tracers during wintertime (9<sup>th</sup>  
257 November to 11<sup>th</sup> December 2016) and summertime (22<sup>nd</sup> May to 24<sup>th</sup> June 2017) at the



258 IAP site are summarized in Table 1 and Fig. S1. The average PM<sub>2.5</sub> concentration was  
 259 94.8±64.4 μg m<sup>-3</sup> during the whole winter sampling campaign. The winter sampling  
 260 period was divided as haze (daily PM<sub>2.5</sub> > 75 μg m<sup>-3</sup>) and non-haze days (<75 μg m<sup>-3</sup>).  
 261 The average daily PM<sub>2.5</sub> was 136.7±49.8 and 36.7±23.5 μg m<sup>-3</sup> on haze and non-haze  
 262 days, respectively. Daily PM<sub>2.5</sub> in the summer sampling period was 30.2±14.8 μg m<sup>-3</sup>,  
 263 comparable with that on winter non-haze days.

264 OC concentrations ranged between 3.9-48.8 μg m<sup>-3</sup> (mean: 21.5 μg m<sup>-3</sup>) and 1.8-12.7  
 265 μg m<sup>-3</sup> (mean: 6.4 μg m<sup>-3</sup>) during winter and summer, respectively. They are  
 266 comparable with the OC concentrations in winter (23.7 μg m<sup>-3</sup>) and summer (3.78 μg  
 267 m<sup>-3</sup>) in Tianjin, China during an almost simultaneous sampling period (Fan et al., 2020),  
 268 but much lower than the OC concentration (17.1 μg m<sup>-3</sup>) in summer 2007 in Beijing  
 269 (Yang et al., 2016). The average OC concentration during haze days (29.4±9.2 μg m<sup>-3</sup>)  
 270 was approximately three times that of non-haze days (10.7±6.2 μg m<sup>-3</sup>) during winter.  
 271 The average EC concentration during winter was 3.5±2.0 μg m<sup>-3</sup>; its concentration was  
 272 4.6±1.3 μg m<sup>-3</sup> on haze days, approximately 2.4 times that on winter non-haze days  
 273 (1.9±1.6 μg m<sup>-3</sup>) and 5 times that (0.9±0.4 μg m<sup>-3</sup>) during the summer sampling period.  
 274 The OC and EC concentrations in this study were comparable with the OC (27.9 ± 23.4  
 275 μg m<sup>-3</sup>) and EC (6.6 ± 5.1 μg m<sup>-3</sup>) concentrations in winter Beijing in 2016 (Qi et al.,  
 276 2018), but much lower than those in an urban area of Beijing during winter (OC and  
 277 EC: 36.7±19.4 and 15.2±11.1 μg m<sup>-3</sup>) and summer (10.7±3.6 and 5.7±2.9 μg m<sup>-3</sup>) in  
 278 2002 (Dan et al., 2004).

279 On average, OC and EC concentrations in winter were 3.3 and 3.9 times those in  
 280 summer. Additionally, OC and EC were well-correlated in this study, with R<sup>2</sup> values of  
 281 0.85 and 0.63 during winter and summer, respectively, suggesting similar sources of  
 282 carbonaceous aerosols, especially in winter. Less correlated OC and EC in summer  
 283 could be a result of SOC formation. SOC in this study was estimated and is discussed  
 284 in section 3.3.7.

285 **Table 1.** Summary of measured concentrations at IAP site in winter and summer.

Compounds <sup>a</sup> / ng m <sup>-3</sup>	Winter		Winter (n=31)	Summer (n=34)
	Haze <sup>a</sup> (n=18)	Non-haze <sup>a</sup> (n=13)		
PM <sub>2.5</sub> (μg m <sup>-3</sup> )	136.7±49.8 (80.5-239.9) <sup>b</sup>	36.7±23.5 (10.3-72)	94.8±64.4 (10.3-239.9)	30.2±14.8 (12.2-78.8)
OC (μg m <sup>-3</sup> )	29.4±9.2 (13.7-48.8)	10.7±6.2 (3.9-21.5)	21.5±12.3 (3.9-48.8)	6.4±2.3 (1.8-12.7)
EC (μg m <sup>-3</sup> )	4.6±1.3 (1.6-6.6)	1.9±1.6 (0.3-5.2)	3.5±2.0 (0.3-6.6)	0.9±0.4 (0.2-1.7)
SOC <sup>c</sup> (μg m <sup>-3</sup> )	10.3±5.7 (2.9-24.6)	2.9±1.4 (0.0-5.5)	7.2±5.7 (0.0-24.6)	2.3±1.4 (0.0-6.0)
Levoglucosan	348.2±148.0 (83.1-512.5)	195.0±163.7 (19.1-539.5)	278.5±171.4 (19.1-539.5)	26.1±28.3 (2.9-172.2)
Palmitic acid	376.2±234.9 (44.5-1089.6)	278±280.6 (33.8-1137.2)	335±255.3 (33.8-1137.2)	25.2±11.9 (9.4-68)
Stearic acid	207.1±181.4 (23-846.7)	163.6±228.1 (17.3-903.2)	188.8±199.8 (17.3-903.2)	16.0±7.2 (5.6-36.4)
Phenanthrene	8.6±6.1 (1.8-19)	5.6±6.1 (1-24.8)	7.3±6.2 (1-24.8)	0.7±0.7 (0-3.8)
Fluoranthene	25.1±19.6 (4.2-76.2)	16.1±21.3 (4.2-84.3)	21.3±20.5 (4.2-84.3)	0.4±0.2 (0-0.9)
Retene	16±14.9 (2-52.2)	11.1±12.1 (0.5-45.5)	13.9±13.8 (0.5-52.2)	0±0 (0-0.1)
Benz(a)anthracene	21.5±16.5 (0.3-62.7)	10.8±9.3 (1.4-30.5)	17±14.8 (0.3-62.7)	0.2±0.1 (0-0.5)
Chrysene	22.6±14.1 (3.7-47.3)	13.6±15.6 (0.1-59.5)	18.8±15.2 (0.1-59.5)	0.2±0.1 (0-0.3)
Benzo(b)fluoranthene	52.6±29 (10.7-98)	28.1±31 (2.4-113.6)	42.3±31.8 (2.4-113.6)	0.7±0.5 (0-2)
Benzo(k)fluoranthene	12.2±8 (0-25.3)	6.7±6.8 (0-23.7)	9.9±7.9 (0-25.3)	0.2±0.1 (0-0.4)
Picene	0.8±0.8 (0-2.6)	0.3±0.5 (0-1.3)	0.6±0.7 (0-2.6)	0±0 (0-0)
Benzo(ghi)perylene	7.0±4.7 (0-13.6)	4.0±4.1 (0-14.0)	5.6±4.6 (0-14.0)	0±0.1 (0-0.3)
17a (H) -22, 29, 30- Trisnorhopane	2.7±1.6 (0.6-6.7)	1.6±1.5 (0.3-6)	2.2±1.6 (0.3-6.7)	0±0.1 (0-0.4)
17b (H), 21a (H) - Norhopane	3.1±1.6 (0.9-6.6)	1.8±1.8 (0.3-7.3)	2.6±1.8 (0.3-7.3)	0±0 (0-0.2)



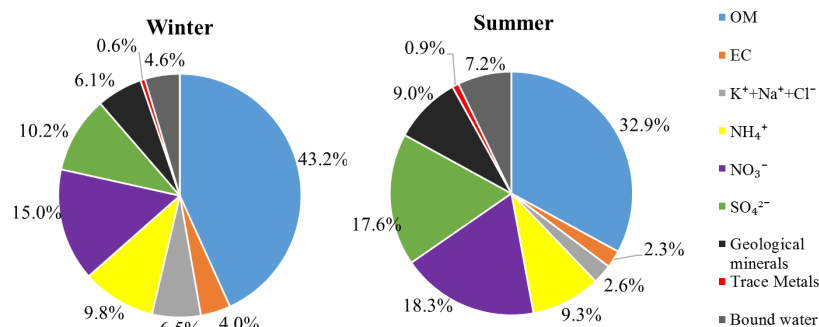


C24	26.3±15.3 (7.8-55.5)	18±19.2 (2.1-71.2)	22.5±17.4 (2.1-71.2)	1.4±0.6 (0.5-3.3)
C25	28.2±15.6 (8.5-59)	19.5±20.5 (2.3-76.2)	24.2±18.3 (2.3-76.2)	2.9±1.5 (0.5-6.5)
C26	18.9±10.2 (5.8-40.2)	13±13.1 (1.8-48.2)	16.2±11.8 (1.8-48.2)	1.6±0.7 (0.3-4.3)
C27	20.4±9.2 (6.1-37.1)	13.8±12.5 (2.2-43.5)	17.4±11.2 (2.2-43.5)	4.4±2 (0.6-11.7)
C28	10.6±4.8 (3.2-19.2)	6.9±5.7 (1.5-19.3)	8.9±5.5 (1.5-19.3)	1.4±0.6 (0.3-2.9)
C29	22.3±10.1 (5.9-39.7)	14.3±12.6 (3-39)	18.7±11.9 (3-39.7)	5.2±3.3 (0.4-20.7)
C30	6.8±2.9 (2.2-11.4)	4.5±3.1 (1-9.7)	5.7±3.2 (1-11.4)	1±0.4 (0.2-2)
C31	11.6±4.2 (3.5-17.7)	7.7±5.8 (1.2-18.7)	9.8±5.3 (1.2-18.7)	4.3±3.2 (0.4-20)
C32	6.1±2.6 (1.7-9.3)	3.9±2.6 (0.7-8.2)	5.1±2.8 (0.7-9.3)	0.9±0.4 (0.2-1.7)
C33	5.8±2.7 (1.7-11.5)	3.9±3.1 (0.9-9.6)	4.9±3 (0.9-11.5)	1.8±1.1 (0.1-6.3)
C34	2.1±2.1 (0-5.5)	1.2±1.4 (0-4)	1.7±1.8 (0-5.5)	0.3±0.3 (0-0.9)

286 <sup>a</sup> The unit is ng m<sup>-3</sup> for all organic compounds and µg m<sup>-3</sup> for PM<sub>2.5</sub>, OC, EC and SOC; <sup>b</sup> mean±SD  
 287 (min-max); <sup>c</sup> SOC concentration was calculated by EC-tracer method; <sup>d</sup> Haze days: PM<sub>2.5</sub>≥75 µg  
 288 m<sup>-3</sup>; <sup>e</sup> Non-haze days: PM<sub>2.5</sub><75 µg m<sup>-3</sup>;

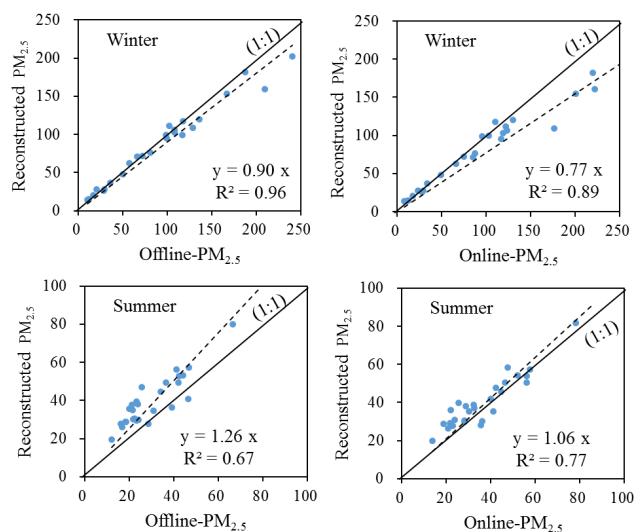
### 289 3.2 Chemical Mass Closure (CMC)

290 The composition of PM<sub>2.5</sub> applying the chemical mass closure method is plotted in Fig.2  
 291 and summarized in Table S1. Because the gravimetrically measured mass (offline PM<sub>2.5</sub>)  
 292 differs slightly from online PM<sub>2.5</sub> (Fig. S2), the regression analysis results between mass  
 293 reconstructed using mass closure (reconstructed PM<sub>2.5</sub>) and both measured PM<sub>2.5</sub>  
 294 (offline PM<sub>2.5</sub>/ online PM<sub>2.5</sub>) were investigated and plotted in Fig. 3.  
 295



296  
 297 **Figure 2.** Chemical components of reconstructed PM<sub>2.5</sub> (offline) applying mass closure method.

298  
 299



300

301

302

**Figure 3.** Regression results between reconstructed  $\text{PM}_{2.5}$  and offline/online  $\text{PM}_{2.5}$  by chemical mass closure method.

303

304

305

306

307

308

309

310

311

312

313

314

315

316

As shown in Fig. 3, measured offline/online  $\text{PM}_{2.5}$  generally agrees well with the reconstructed  $\text{PM}_{2.5}$ . In winter, the regression results were good between reconstructed  $\text{PM}_{2.5}$  and offline- $\text{PM}_{2.5}$ . For online- $\text{PM}_{2.5}$ , it was much higher than the reconstructed  $\text{PM}_{2.5}$  when the mass was over  $170 \mu\text{g m}^{-3}$ . After excluding the outliers (2 outliers of offline- $\text{PM}_{2.5} > 200 \mu\text{g m}^{-3}$  and 4 outliers of online- $\text{PM}_{2.5} > 170 \mu\text{g m}^{-3}$ ), the regression results improved with both slopes and  $R^2$  approaching unity (Fig. S3). This could indicate some uncertainties in offline and online  $\text{PM}_{2.5}$  measurement for heavily polluted samples. During the summer campaign, the slope of the reconstructed  $\text{PM}_{2.5}$  and online- $\text{PM}_{2.5}$  was close to 1, but that of reconstructed  $\text{PM}_{2.5}$  and offline- $\text{PM}_{2.5}$  was 1.26. This could be due to the positive artifacts of quartz filters for chemical analyses, which can absorb more organics than PTFE filters that are used for PM weighing. The datapoints were more scattered in summer, which could result from the large difference in OM-OC relationships from day to day. The reconstructed inorganics (reconstructed  $\text{PM}_{2.5}$  excluding OM) correlated well with offline- $\text{PM}_{2.5}$ , but OM did not (Fig. S4).

317

318

319

320

321

322

323

During the winter campaign, the carbonaceous components (OM & EC) accounted for 47.2% of total reconstructed  $\text{PM}_{2.5}$ , followed by the secondary inorganic ions ( $\text{NH}_4^+$ ,  $\text{SO}_4^{2-}$ ,  $\text{NO}_3^-$ ) (35.0%). In summer, on the contrary, secondary inorganic salts represented 45.2% of  $\text{PM}_{2.5}$  mass, followed by carbonaceous components (35.2%). Bound water contributed 4.6% and 7.2% of  $\text{PM}_{2.5}$  during the winter and summer, respectively. All other components combined accounted for 13.2% and 12.4% of  $\text{PM}_{2.5}$  during the winter and summer campaigns, respectively.

324

325

### 3.3 Source apportionment of fine OC in urban Beijing applying a CMB model

326

327

The CMB model resolved seven primary sources of OC in winter and summer, including vegetative detritus, straw and wood burning (biomass burning, BB), gasoline



328 vehicles, diesel vehicles, industrial coal combustion (Industrial CC), residential coal  
329 combustion (Residential CC) and cooking. It explained an average of 75.7% (45.3-  
330 91.3%) and 56.1% (34.3-76.3%) of fine OC in winter and summer, respectively. The  
331 averaged CMB source apportionment results in winter and summer are presented in  
332 Table 2. Daily source contribution estimates to fine OC and the relative abundance of  
333 different sources contributions to OC in winter and summer are shown in Fig. 4.

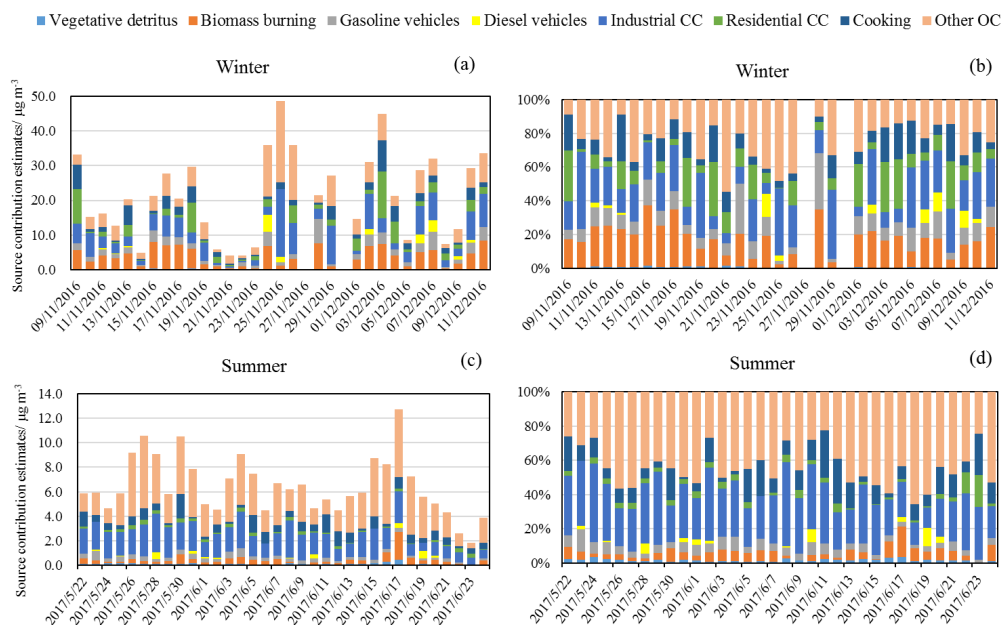
334 During the winter campaign, coal combustion (industrial and residential CC,  $7.5 \mu\text{g m}^{-3}$ ,  
335  $35.0\%$  of OC) was the most significant contributor to OC, followed by Other OC  
336 ( $5.3 \mu\text{g m}^{-3}$ ,  $24.8\%$ ), biomass ( $3.8 \mu\text{g m}^{-3}$ ,  $17.6\%$ ), traffic (gasoline and diesel vehicles,  
337  $2.6 \mu\text{g m}^{-3}$ ,  $11.9\%$ ), cooking ( $2.2 \mu\text{g m}^{-3}$ ,  $10.3\%$ ), vegetative detritus ( $0.09 \mu\text{g m}^{-3}$ ,  $0.4\%$ ).  
338 On winter haze days, industrial coal combustion, cooking and Other OC were  
339 significantly higher (nearly tripled) compared to non-haze days. During the summer  
340 campaign, Other OC ( $2.9 \mu\text{g m}^{-3}$ ,  $45.6\%$ ) was the most significant contributor to OC,  
341 followed by coal combustion ( $2.0 \mu\text{g m}^{-3}$ ,  $31.1\%$ ), cooking ( $0.7 \mu\text{g m}^{-3}$ ,  $10.3\%$ ), traffic  
342 ( $0.4 \mu\text{g m}^{-3}$ ,  $6.1\%$ ), biomass burning ( $0.3 \mu\text{g m}^{-3}$ ,  $5.3\%$ ), and vegetative detritus ( $0.1 \mu\text{g}$   
343  $\text{m}^{-3}$ ,  $1.7\%$ ).

344 **Table 2.** Source contribution estimates (SCE,  $\mu\text{g m}^{-3}$ ) for fine OC in urban Beijing  
345 during winter and summer from the CMB model

Sources	Winter		Winter (n=31)	Summer (n=34)
	Haze (n=18)	Non-haze (n=13)		
Vegetative detritus	0.11±0.08	0.07±0.08	0.09±0.08	0.11±0.08
Biomass burning	4.80±2.23	2.38±2.57	3.78±2.64	0.34±0.39
Gasoline vehicles	2.35±1.27	1.59±1.85	2.03±1.56	0.31±0.16
Diesel vehicles	0.83±1.43	0.14±0.33	0.54±1.15	0.08±0.16
Industrial coal combustion	7.09±4.17	1.95±1.36	4.94±4.15	1.82±0.72
Residential coal combustion	3.64±3.72	1.16±0.96	2.60±3.12	0.18±0.11
Cooking	3.23±2.30	0.85±0.52	2.23±2.13	0.66±0.43
Other OC <sup>a</sup>	7.4±5.6	2.5±1.4	5.3±4.9	2.9±1.5
Calculated OC <sup>b</sup>	22.0±6.5	8.2±5.3	16.2±9.1	3.5±1.2
Measured OC	29.4±9.2	10.7±6.2	21.5±12.3	6.4±2.3

346 <sup>a</sup> Other OC is calculated by subtracting calculated OC from measured OC;

347 <sup>b</sup> Calculated OC is the sum of OC from all seven primary sources: vegetative detritus, biomass burning,  
348 gasoline vehicles, diesel vehicles, industrial coal combustion, residential coal combustion and cooking.



349

350 **Figure 4.** Daily source contribution estimates to fine OC in (a) winter and (c) summer  
351 and their relative abundance in winter (b) and summer (d)



### 3.3.1 Industrial and residential coal combustion

In China, a large amount of coal is used in thermal power plant, industries, urban and rural houses in northern China, especially during the heating period (mid-November to mid-March) (Huang et al., 2017; Yu et al., 2019). But urban household coal use experienced a remarkable drop of 58% during 2005-2015, which is much higher than that of rural household coal use (5% of decrease) (Zhao et al., 2018). In this study, coal combustion is the single largest contributor to primary OC in both winter and summer. In addition, industrial CC was a more significant source of OC than residential CC in urban Beijing. On average, coal combustion related OC was  $7.5 \pm 5.0 \mu\text{g m}^{-3}$  ( $34.5 \pm 9.8\%$  of OC) in winter, which was more than 3 times of that in summer -  $2.0 \pm 0.8 \mu\text{g m}^{-3}$  ( $32.3 \pm 10.2\%$  of OC), but the percentage contribution is similar. A similar seasonal trend was also found in other studies in Beijing (Zheng et al., 2005; Wang et al., 2009), but the relative contribution of coal combustion was much lower than in this study. Industrial CC derived OC was  $4.94 \pm 4.15$  and  $1.82 \pm 0.72 \mu\text{g m}^{-3}$  in winter and summer, respectively. Residential CC derived OC was  $2.60 \pm 3.12$  and  $0.18 \pm 0.11 \mu\text{g m}^{-3}$  in winter and summer, respectively. Residential CC was much higher in winter compared to that in summer. On haze days, industrial CC and residential CC derived OC were 3.6 and 3.1 times that on non-haze days, respectively, indicating an important contribution to haze formation from industrial CC.

Chloride has been considered as a tracer for coal combustion (Chen et al., 2014). The time series of OC from coal combustion (OC-CC) and  $\text{Cl}^-$  during winter and summer of Beijing are shown in Fig. 5. OC-CC and  $\text{Cl}^-$  exhibited similar trends in both seasons. The correlation coefficient ( $R^2$ ) between OC-CC and  $\text{Cl}^-$  during winter was 0.62 but there is no significant correlation between the two during the summer campaign while. This is probably related to the semi-volatility of ammonium chloride, which is liable to evaporate in summer (Pio and Harrison, 1987). A similar phenomenon has been observed in Delhi (Pant et al., 2015).

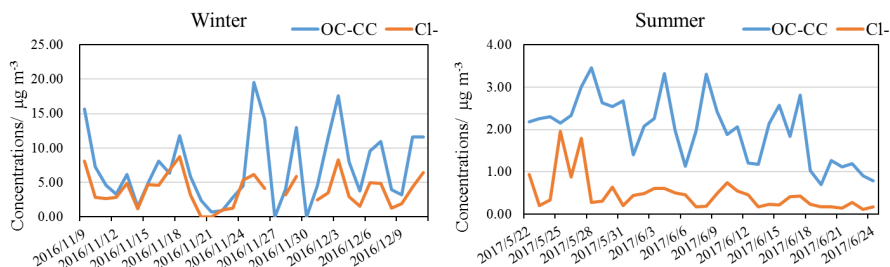


Figure 5. Time series of OC from coal combustion (OC-CC) and  $\text{Cl}^-$  in winter and summer in Beijing

### 3.3.2 Biomass burning

Biomass burning (BB), including straw and wood burning, is an important source of atmospheric fine OC, which ranked as the second highest primary source of OC, after industrial coal combustion during the winter campaign, and third highest during the summer campaign after industrial CC and cooking. As shown in Fig. 4, the relative



388 abundance of BB derived-OC during the winter campaign is much higher than the  
389 summer campaign. BB-derived OC from the CMB results was  $3.78\pm 2.64 \mu\text{g m}^{-3}$  and  
390  $0.34\pm 0.39 \mu\text{g m}^{-3}$  in winter and summer, contributing 17.6% and 5.3% of OC in these  
391 two seasons, respectively. These results are lower than those in 2005-2007 Beijing  
392 when BB accounted for 26% and 11% of OC in winter and summer, respectively (Wang  
393 et al., 2009). The BB-derived OC on winter haze days ( $4.80\pm 2.23 \mu\text{g m}^{-3}$ ) was  
394 approximately double that of non-haze days ( $2.38\pm 2.57 \mu\text{g m}^{-3}$ ), accounting for 16.3%  
395 and 22.2% of OC on haze and non-haze days, respectively.

396 Levoglucosan is widely used as a key tracer for biomass burning emissions (Bhattarai  
397 et al., 2019; Cheng et al., 2013; Xu et al., 2019a). Based on a levoglucosan to OC ratio  
398 of 8.2 % (Zhang et al., 2007a; Fan et al., 2020), the BB-derived OC was  $3.40\pm 2.09 \mu\text{g}$   
399  $\text{m}^{-3}$  and  $0.32\pm 0.35 \mu\text{g m}^{-3}$  during the winter and summer campaigns, respectively. These  
400 results are comparable to BB-derived OC from the CMB in this study. The estimated  
401 BB-derived OC concentration are also comparable with the BB-derived OC during the  
402 same sampling periods in Tianjin (Fan et al., 2020), but higher than those at IAP in  
403 2013-2014 (Kang et al., 2018).. Both of the studies applied the levoglucosan/OC ratio  
404 method to estimate the BB-derived OC although the actual ratio in Beijing air may be  
405 very different to 8.2%. The heavily elevated OC concentration in winter compared to  
406 summer could be a result of increased biomass burning activities for house heating and  
407 cooking in Beijing in addition to the unfavorable dispersion conditions under stagnant  
408 weather conditions in the winter.

409 In summer, the total OC concentration was highest on 17<sup>th</sup> June. The sudden rise of  
410 OC on this day was attributed to the enhanced biomass burning activities, which led to  
411 the highest level of BB-derived OC and highest BBOC to OC abundance. The  
412 levoglucosan concentration on this day was also the highest in summer, which reached  
413  $172 \text{ ng m}^{-3}$ .

### 414 3.3.3 Gasoline and diesel vehicles

415 OC and EC are the key components of traffic emissions (gasoline vehicles & diesel  
416 engines) (Chen et al., 2014; Chuang et al., 2016). Traffic related OC, as represented by  
417 the total sum of OC from gasoline and diesel vehicles, was  $2.4\pm 2.3$  and  $0.39\pm 0.22 \mu\text{g}$   
418  $\text{m}^{-3}$ , and contributed  $12.1\pm 7.8\%$  and  $6.1\pm 3.3\%$  of OC in winter and summer,  
419 respectively. These results are lower than the contribution of vehicle emissions to OC  
420 (13-20%) in Beijing during 2005 and 2006 (Wang et al., 2009), suggesting traffic  
421 emissions may be a less significant contributor to fine OC in the atmosphere in Beijing  
422 in 2016/2017. By multiplying by OM/OC factors of 2.39 and 1.47 in winter and summer,  
423 respectively, as mentioned in section 2.3, traffic related organic aerosol contributed  
424  $8.2\pm 6.5\%$  and  $2.3\pm 1.7\%$  of  $\text{PM}_{2.5}$  in winter and summer, respectively. The summer  
425 result was comparable with the vehicular emissions contribution to  $\text{PM}_{2.5}$  (2.1%) in  
426 summer in Beijing, but higher than that in winter (1.5%) in Beijing estimated by using  
427 a PMF model (Yu et al., 2019). Gasoline vehicles dominated the traffic emissions;  
428 gasoline vehicle-derived OC was  $2.03\pm 1.56$  and  $0.31\pm 0.16 \mu\text{g m}^{-3}$  in winter and  
429 summer, respectively, which are approximately four times than that in winter  
430 ( $0.54\pm 1.15 \mu\text{g m}^{-3}$ ) and summer ( $0.08\pm 0.16 \mu\text{g m}^{-3}$ ) attributed to diesel vehicles. On  
431 haze days, gasoline- and diesel-derived OC were  $2.35\pm 1.27$  and  $0.83\pm 1.43 \mu\text{g m}^{-3}$ ,  
432 respectively, much higher than gasoline- ( $1.59\pm 1.85 \mu\text{g m}^{-3}$ ) and diesel-derived  
433 ( $0.14\pm 0.33 \mu\text{g m}^{-3}$ ) OC on non-haze days. Even though diesel vehicles played a less



434 important role in OC emissions, diesel-derived OC on haze days increased by around 6  
435 times above that of non-haze days, and such an increase was much higher than for  
436 gasoline, suggesting a potentially important role of diesel emissions on haze formation.

### 437 3.3.4 Cooking

438 Cooking is expected to be an important contributor of fine OC in densely populated  
439 Beijing, which has a population of over 21 million. The cooking source profile was  
440 selected from a study which was carried out in the urban area of another Chinese  
441 megacity- Guangzhou, which includes fatty acids, sterols, monosaccharide anhydrides,  
442 alkanes and PAHs in particles from the Chinese residential cooking (Zhao et al., 2015).  
443 The resultant cooking related OC concentrations were  $2.23 \pm 2.13 \mu\text{g m}^{-3}$  and  $0.66 \pm 0.43$   
444  $\mu\text{g m}^{-3}$  in winter and summer, respectively, and both accounted for about 10% to total  
445 OC. Cooking OC was  $3.23 \pm 2.30 \mu\text{g m}^{-3}$  on winter haze days, around four times higher  
446 than that on non-haze days ( $0.85 \pm 0.52 \mu\text{g m}^{-3}$ ).

### 447 3.3.5 Vegetative detritus

448 Vegetative detritus made a minor contribution to fine particle mass. Its concentration  
449 was  $0.09 \pm 0.08 \mu\text{g m}^{-3}$  (0.4%) and  $0.11 \pm 0.08 \mu\text{g m}^{-3}$  (1.7%) of OC during the winter and  
450 summer campaigns, respectively. These contributions are comparable with that in  
451 winter (0.5%), but higher than that in summer (0.3%) in urban Beijing during 2006-  
452 2007 (Wang et al., 2009). These results are also higher than the plant debris-derived  
453 OC in Tianjin in winter 2016 ( $0.02 \mu\text{g m}^{-3}$ ) and summer 2017 ( $0.01 \mu\text{g m}^{-3}$ ), which were  
454 calculated based on the relationship of glucose and plant debris and a OM/OC ratio of  
455 1.93 (Fan et al., 2020).

### 456 3.3.6 Other OC

457 The Other OC was calculated by subtracting the calculated OC (the sum of OC from  
458 seven main sources) from measured OC concentrations. As shown in Table S2, there  
459 are four major source categories of OC in Beijing based on the Multi-resolution  
460 Emission Inventory for China (MEIC), which include power, industry, residential and  
461 transportation (Zheng et al., 2018). In the “industry” category, industrial coal  
462 combustion has been resolved by the CMB model. The local emissions of OC from  
463 industrial coal in Beijing were zero (shown in Table S2), and hence, the resolved POC  
464 from industrial coal combustion in Beijing should be regionally-transported. The MEIC  
465 data also show a small industrial oil combustion source. Since the tracers for this are  
466 likely to be the same as those for petroleum-derived road traffic emissions in CMB, this  
467 may result in a small overestimation of the latter source. For the industrial processes  
468 related OC which have not been resolved by the CMB model, the annual average OC  
469 emissions in Beijing were 1161 and 1083 tonnes in 2016 and 2017 respectively, which  
470 accounted for 7.7% and 9.0% of the total OC emissions (POC). Therefore, the  
471 contribution from industrial processes to the total OC in the atmosphere (POC+SOC)  
472 was considered relatively small. The Other OC in this study is likely to be a mixture of  
473 predominantly SOC and a small portion of POC from sources such as industrial  
474 processes.



475 The Other OC was  $5.3 \pm 4.9$  and  $2.9 \pm 1.5$   $\mu\text{g m}^{-3}$  in winter and summer, respectively,  
476 contributing 24.8% and 43.9% of total measured OC. This is in good agreement with  
477 the Other OC estimated by CMB in another study in urban Beijing, for which Other OC  
478 contributed 22% and 44% of OC in winter and summer, respectively (Wang et al., 2009).  
479 SOC/OC in summer was more than 10% higher than that in summer 2008 in Beijing  
480 estimated using a tracer yield method, with the SOC derived from specific VOC  
481 precursors (toluene, isoprene,  $\alpha$ -pinene and  $\beta$ -caryophyllene) accounting for 32.5% of  
482 OC (Guo et al., 2012).

483 Even though the Other OC concentration was lower in summer, its relative  
484 abundance was higher than that in winter, suggesting relatively higher efficiency of  
485 SOA formation in summer due to more active photochemical processes under higher  
486 temperature and strong radiation. The Other OC on winter haze days was  $7.4 \pm 5.6$   $\mu\text{g}$   
487  $\text{m}^{-3}$ , approximately 3 times of that on non-haze days ( $2.5 \pm 1.4$   $\mu\text{g m}^{-3}$ ). Other OC is also  
488 compared with the SOC estimated by EC-tracer method below.

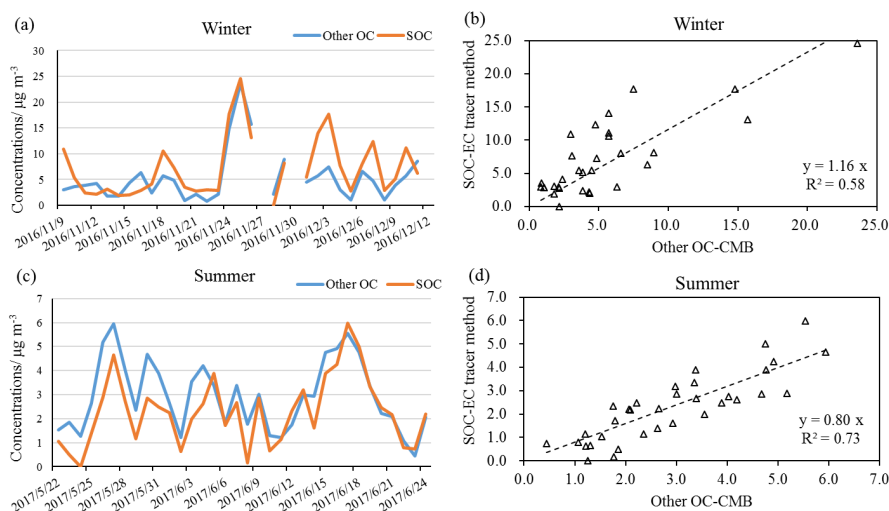
### 489 3.3.7 SOC calculated based on the EC-tracer method

490 EC is a primary pollutant, while OC can originate from both primary sources and form  
491 in the atmosphere from gaseous precursors, namely primary organic carbon (POC) and  
492 SOC, respectively (Xu et al., 2018). The OC/EC ratios can be used to estimate the  
493 primary and secondary carbonaceous aerosol contributions. Usually, OC/EC ratios  $>$   
494 2.0 or 2.2 have been applied to identify and estimate SOA (Liu et al., 2017). In this  
495 study, all samples were observed with higher OC/EC ratios ( $>2.2$ ). SOC in this study  
496 was estimated using the equation below, assuming EC comes 100% from primary  
497 sources and the OC/EC ratio in primary sources is relatively constant (Turpin and  
498 Huntzicker, 1995; Castro et al., 1999):

$$499 \text{SOC}_i = \text{OC}_i - \text{EC}_i \times (\text{OC/EC})_{\text{pri}} \quad (4)$$

500 where  $\text{SOC}_i$ ,  $\text{OC}_i$  and  $\text{EC}_i$  are the ambient concentrations of secondary organic  
501 carbon, organic carbon and elemental carbon of sample  $i$ , respectively.  $(\text{OC/EC})_{\text{pri}}$  is  
502 the OC/EC ratio in primary aerosols. It is difficult to accurately determining the ratio  
503 of  $(\text{OC/EC})_{\text{pri}}$  for a given area.  $(\text{OC/EC})_{\text{pri}}$  varies with the contributions of different  
504 sources and can also be influenced by meteorological conditions (Dan et al., 2004). In  
505 this work,  $(\text{OC/EC})_{\text{pri}}$  was determined based on the lowest 5% of measured OC/EC  
506 ratios for the winter and summer campaigns, respectively (Pio et al., 2011). The average  
507 SOC concentrations during summer and winter were calculated and are shown in Table  
508 1. Daily concentrations of Other OC estimated by CMB and SOC estimated by the EC-  
509 tracer method in winter and summer are plotted in Fig. 6, as well as their correlation  
510 relationship.





511  
512 **Figure 6.** Time series of mean values for Other OC estimated by CMB and SOC  
513 estimated by the EC-tracer method in winter (a) and summer (c); Correlation  
514 relationship between Other OC estimated by CMB and SOC estimated by the EC-tracer  
515 method in winter (b) and summer (d).

516 The average SOC concentrations in winter and summer are presented in Table 1. The  
517 average SOC concentration during winter was  $7.2 \pm 5.7 \mu\text{g m}^{-3}$ , accounted for  
518  $36.6 \pm 15.9\%$  of total OC. The average SOC concentration during summer was one third  
519 of that in winter, which was  $2.3 \pm 1.4 \mu\text{g m}^{-3}$ , accounting for  $36.2 \pm 16.0\%$  of total OC.  
520 The mean SOC concentrations during winter haze and non-haze periods were  $10.3 \pm 5.7$   
521  $\mu\text{g m}^{-3}$  and  $2.9 \pm 1.4 \mu\text{g m}^{-3}$ , contributing to  $34.0 \pm 12.0\%$  and  $40.5 \pm 20.4\%$  of OC during  
522 haze and non-haze episodes, respectively. As shown in Fig. 6, the SOC estimated by  
523 the EC tracer method followed a similar trend to the Other OC calculated by the CMB  
524 model. They were well-correlated in both seasons with  $R^2$  of 0.58 and 0.73 in winter  
525 and summer samples, respectively and gradients of 1.16 and 0.80. This suggests that  
526 the estimates of Other OC calculated from the CMB outputs were reasonable and  
527 mainly represented the secondary organic aerosol.

### 528 3.4 Comparison with the source apportionment results in rural Beijing

529 The OC source apportionment results in this study are also compared with those in  
530 another study conducted at a rural site of Beijing - Pinggu during APHH-Beijing  
531 campaigns (Wu et al., 2020). CMB was run based on the results from high-time  
532 resolution  $\text{PM}_{2.5}$  samples that were collected in Pinggu during the same sampling period,  
533 but not on identical days. The comparison results are presented in Table 3.

534 As shown in Table 3, slightly more OC was explained by CMB at the urban site  
535 ( $75.7\%$ ) than the rural site ( $69.1\%$ ) during winter, but less OC was explained at the  
536 urban site ( $56.1\%$ ) than the rural site ( $63.4\%$ ) during summer. As at the urban site,  
537 biomass burning and coal combustion are important primary sources in rural Beijing.  
538 Diesel contributed more to OC at the rural site, while cooking contributed more at the  
539 urban site. The rural site also had a larger contribution from vegetative detritus to OC  
540 than the urban site. The source contribution estimates from biomass burning at the rural



541 site was approximately 2 and 4 times that at the urban site during winter and summer.  
 542 In winter, biomass burning contributed a similar percentage of OC at both sites. A  
 543 higher percentage of OC from biomass burning was found at the rural site than the  
 544 urban site in summer, possibly because of use of biomass for cooking. For traffic  
 545 emitted OC, gasoline exceeded diesel at the urban site, while the rural site by contrast  
 546 has a larger diesel contribution. Industrial CC emitted OC is higher at the urban site  
 547 during winter, but lower in summer compared to the rural site. The source contribution  
 548 estimates of residential CC at the urban site is only half that of the rural site in both  
 549 seasons, and its relative contribution to OC was also lower at the urban site. Coal is  
 550 widely used for cooking and heating at the villages around the rural site at the time of  
 551 observations. Cooking accounted for over 10% of OC at the urban site, but less than 5%  
 552 at the rural site, which is plausible as the urban site is more densely populated.

553 **Table 3.** Comparison of the source contribution estimates (SCE in  $\mu\text{g m}^{-3}$  (%OC)) at  
 554 IAP with those at a rural site in Beijing- Pinggu

	IAP (Urban) (This study)		Pinggu (Rural)	
	Winter (31 days)	Summer (34 days)	Winter (14 days)	Summer (6 days)
OC	21.5±12.3	6.4±2.3	36.5±29.3	10.7±4.9
OC explained	75.7±11.0%	56.1±11.3%	69.1±7.1%	63.4±12.6%
Vegetative detritus	0.1±0.1 (0.5±0.4%)	0.1±0.1 (1.7±0.8%)	1.5±3.0 (2.8±3.4%)	0.3±0.3 (2.1±1.4%)
Biomass burning	3.8±2.6 (17.4±8.7%)	0.3±0.4 (4.8±3.4%)	6.8±5.6 (18.1±3.4%)	1.1±0.6 (10.7±2.6%)
Gasoline	2.0±1.6 (10.2±6.6%)	0.3±0.2 (4.9±2.2%)	1.0±0.9 (3.4±1.6%)	0.1±0.0 (1.3±0.6%)
Diesel	0.5±1.2 (1.9±3.7%)	0.1±0.2 (1.2±2.5%)	6.2±6.0 (13.7±6.0%)	0.6±0.3 (6.2±4.8%)
Industrial CC	4.9±4.1 (22.0±11.2%)	1.8±0.7 (29.0±9.0%)	3.2±2.6 (10.2±5.7%)	3.8±2.5 (34.1±11.0%)
Residential CC	2.6±3.1 (12.5±10.2%)	0.2±0.1 (3.3±3.5%)	5.7±4.3 (19.0±12.4%)	0.4±0.2 (4.2±1.8%)
Cooking	2.2±2.1 (10.6±7.3%)	0.7±0.4 (11.1±7.1%)	0.5±0.5 (2.0±2.3%)	0.5±0.4 (4.9±3.9%)
Other OC	5.3±4.9 (24.8±12.1%)	2.9±1.5 (43.9±11.4%)	11.7±10.4 (30.9±7.1%)	3.9±2.3 (36.6±12.6%)

### 555 3.5 Comparison with source apportionment results from AMS-PMF

556 Results from AMS-PMF were compared with the CMB source apportionment results  
 557 to investigate the consistency and potential uncertainties of both methods, and also to  
 558 provide supplemental source apportionment results. Six factors in non-refractory (NR)-  
 559  $\text{PM}_{10}$  from the AMS were identified based on the mass spectra measured in winter at  
 560 IAP by applying a PMF model, including coal combustion OA (CCOA), cooking OA  
 561 (COA), biomass burning OA (BBOA) and 3 secondary factors of oxidized primary OA  
 562 (OPOA), less-oxidized OA (LOOOA), and more-oxidized OA (MOOOA). In summer,  
 563 the PMF analysis resulted in 5 factors including 2 primary factors of hydrocarbon-like  
 564 OA (HOA), cooking OA (COA) and 3 secondary factors of oxygenated OA (OOA):  
 565 OOA1, OOA2, OOA3. In order to compare with the source apportionment results of  
 566 OC in this study from the CMB model, the OA concentrations from the AMS-PMF  
 567 were converted to OC based on various OA/OC ratios measured in Beijing: 1.35 for  
 568 CCOA/CCOC (coal combustion organic carbon), 1.31 for HOA/HOC (hydrocarbon-  
 569 like organic carbon) (Sun et al., 2016), 1.38 for COA/COC (cooking organic carbon),  
 570 1.58 for BBOA/BBOC (biomass burning organic carbon) (Xu et al., 2019b), and 1.78  
 571 for OOA/OOC (Huang et al., 2010). The concentrations of OA and corresponding OC  
 572 from AMS-PMF analysis are presented in Table 4.

573 **Table 4.** Source contributions of OA and OC ( $\mu\text{g m}^{-3}$ ) from AMS-PMF results in urban  
 574 Beijing during winter and summer

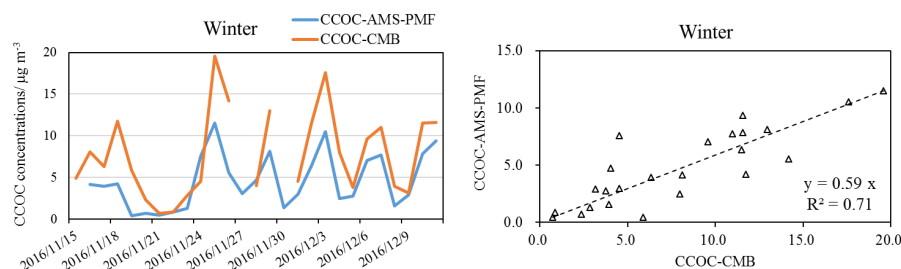
Winter/ $\mu\text{g m}^{-3}$



CCOA	6.2±4.4	CCOC	4.6±3.3
COA	5.9±4.1	COC	4.3±3.0
BBOA	6.5±5.8	BBOC	4.1±3.7
OPOA	4.6±2.1	OPOC	2.6±1.2
LOOOA	5.2±5.2	LOOOC	2.9±2.9
MOOOA	8.1±7.0	MOOOC	4.6±4.0
OOA <sup>a</sup>	18.0±13.2	OOC <sup>d</sup>	10.1±7.4
OM <sup>b</sup>	36.7±24.0		
Summer/ $\mu\text{g m}^{-3}$			
HOA	0.7±0.4	HOC	0.5±0.3
COA	1.8±1.0	COC	1.3±0.7
OOA1	3.3±1.4	OOC1	1.9±0.8
OOA2	2.4±2.4	OOC2	1.4±1.3
OOA3	1.9±1.1	OOC3	1.1±0.6
OOA <sup>c</sup>	7.6±3.7	OOC	4.3±2.1
OM	10.1±3.9		

575 <sup>a</sup> OOA=OPOA+LOOOA+MOOOA; <sup>b</sup> OM is organics measured by AMS; <sup>c</sup> OOA=OOA1+OOA2+OOA3;  
 576 <sup>d</sup> OOC=OOC1+OOC2+OOC3

577 The CCOA factor was mainly characterized by  $m/z$  of 44, 73 and 115 (Sun et al.,  
 578 2016). In winter, CCOA was  $6.2\pm 4.4 \mu\text{g m}^{-3}$ , contributing 16.9% of OM. CCOC was  
 579  $4.6\pm 3.3 \mu\text{g m}^{-3}$ , which was much lower than the estimated coal combustion OC ( $7.5\pm 5.0$   
 580  $\mu\text{g m}^{-3}$ , industrial and residential coal combustion OC) by CMB. The time series of coal  
 581 combustion related OC (CCOC) estimated by CMB and CCOC from AMS-PMF  
 582 analysis in Fig. 7 showed a similar trend with relatively good correlation of  $R^2 = 0.71$ ,  
 583 but coal combustion estimated by CMB was consistently higher than by AMS-PMF,  
 584 probably because AMS-PMF only resolved the sources of NR-PM<sub>1.0</sub>, and some coal  
 585 combustion particles are larger (Xu et al., 2011). The correlation coefficients ( $R^2$ ) of  
 586 CCOC from AMS-PMF with Cl<sup>-</sup> and NR-Cl<sup>-</sup> were 0.49 and 0.65, respectively in the  
 587 winter data.



588  
 589 **Figure 7.** Time series and correlation of coal combustion related OC (CCOC) estimated  
 590 by CMB and CCOC from AMS-PMF analysis

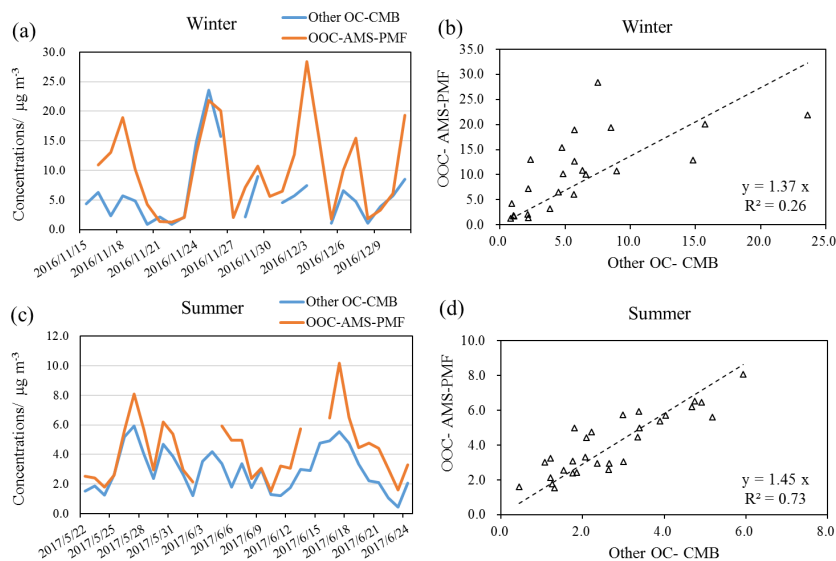
591 BBOA from the AMS data in winter was  $6.5\pm 5.8 \mu\text{g m}^{-3}$ , contributing 17.7% of OM.  
 592 This BBOA factor included a high proportion of  $m/z$  60 and 73, which are typical  
 593 fragments of anhydrous sugars like levoglucosan (Srivastava et al., 2019). BBOC was  
 594  $4.1\pm 3.7 \mu\text{g m}^{-3}$ , which was very close to the estimated BBOC ( $3.78\pm 2.64 \mu\text{g m}^{-3}$ , 17.6%  
 595 of OC) by CMB in this study.



596 COA is as a common factor identified in both winter and summer AMS-PMF results.  
597 It is characterized by high  $m/z$  of 55 and 57 in the mass spectrum (Sun et al., 2016).  
598 COA was  $5.9\pm 4.1$  and  $1.8\pm 1.0 \mu\text{g m}^{-3}$  in winter and summer, respectively, contributing  
599 16.1% and 17.8% of OM. COC was  $4.3\pm 3.0$  and  $1.3\pm 0.7 \mu\text{g m}^{-3}$  in winter and summer,  
600 respectively, which were almost 2 times of those for winter ( $2.23\pm 2.13 \mu\text{g m}^{-3}$ ) and  
601 summer ( $0.66\pm 0.43 \mu\text{g m}^{-3}$ ) in the CMB results.

602 HOA was  $0.7\pm 0.4 \mu\text{g m}^{-3}$  in summer, accounting for 6.9% of OM. HOA is usually  
603 identified based on the high contribution of aliphatic hydrocarbons in this factor,  
604 particularly  $m/z$  of 27, 41, 55, 57, 69 and 71 (Aiken et al., 2009). This result is lower  
605 than that (17% of OM) in rural Beijing during summer 2015 (Hua et al., 2018). HOC  
606 was  $0.5\pm 0.3 \mu\text{g m}^{-3}$  in summer, which is higher than the traffic (gasoline+diesel)  
607 emitted OC ( $0.4\pm 0.2 \mu\text{g m}^{-3}$ ) from the CMB model. No obvious correlation was  
608 observed between HOC with nitrate and traffic emitted OC from the CMB model during  
609 summer.

610 AMS OOA concentrations (the sum of all oxidized OA) were  $18.0\pm 13.2$  and  $7.6\pm 3.7$   
611  $\mu\text{g m}^{-3}$  in winter and summer, respectively, accounting for 49.0% and 75.2% of OM.  
612 The derived OOC concentrations in winter and summer were  $10.1\pm 7.4$  and  $4.3\pm 2.1 \mu\text{g m}^{-3}$   
613  $\mu\text{g m}^{-3}$  in winter and summer, respectively, higher than the Other OC estimated by CMB  
614 in winter ( $5.3\pm 4.9 \mu\text{g m}^{-3}$ ) and summer ( $2.9\pm 1.5 \mu\text{g m}^{-3}$ ) in this study. The time series  
615 and correlation of Other OC estimated by CMB results and OOC from AMS-PMF  
616 results is plotted in Fig. 8. A similar temporal trend was found between them, especially  
617 in summer, which was also observed with a better correlation ( $R^2=0.73$ ).



618  
619 **Figure 8.** Time series of mean values for Other OC estimated by CMB, and OOC  
620 estimated by AMS-PMF in winter (a) and summer (c); Correlation relationship between  
621 Other OC estimated by CMB and OOC estimated by AMS-PMF in winter (b) and  
622 summer (d).



623 In summary, CMB is able to resolve almost all major known primary OA sources, but  
624 AMS-PMF can resolve more secondary OA sources. The AMS-PMF results for major  
625 components, such as CCOC and OOC agreed well with the results from CMB in the  
626 winter. However, discrepancies or poor agreement was found for other sources, such as  
627 BBOA and COA, although the temporal features were very similar. Furthermore, AMS-  
628 PMF did not identify certain sources, probably due to their relatively small contribution  
629 to particle mass. Overall, CMB and AMS-PMF offered complementary data to resolve  
630 both primary and secondary sources.

### 631 **3.6 Source contributions to PM<sub>2.5</sub> from the CMB model**

632 The source contributions to PM<sub>2.5</sub> were calculated by multiplication of the fine OC  
633 source estimates from CMB by the ratios of fine OC to PM<sub>2.5</sub> mass (Table S3), which  
634 were obtained from the same source profiles used for the OC apportionment by CMB  
635 (Zhang et al., 2007b; Wang et al., 2009; Cai et al., 2017; Zhang et al., 2008). For cooking,  
636 an OM/OC ratio of 1.4 was applied (Zhao et al., 2007). For vegetative detritus, OM/OC  
637 ratio of 2.1 was applied (Bae et al., 2006b). The OM/OC ratios for oxygenated OA were  
638 in the range of 1.85-2.3 (Zhang et al., 2005; Aiken et al., 2008), and the OM/OC ratio  
639 was 2.17 in secondary organic aerosols of PM<sub>2.5</sub> (Bae et al., 2006a). Therefore, an  
640 OM/OC ratio of 2.2 is applied in this study to convert the Other OC to OM. Instead of  
641 OC/PM<sub>2.5</sub>, applying an OM/OC ratio for the calculation may result in an  
642 underestimation of PM<sub>2.5</sub> source contributions, because sources like cooking and  
643 vegetative detritus can also emit inorganic pollutants. However, cooking emissions are  
644 mostly organic and the contribution from vegetative detritus to PM<sub>2.5</sub> is very small, their  
645 effects on source contribution estimation here are considered negligible. The daily  
646 PM<sub>2.5</sub> contribution estimates are provided in Fig. 9. The seasonal average source  
647 contributions and their relative abundance in reconstructed PM<sub>2.5</sub> are summarized in  
648 Table S4.

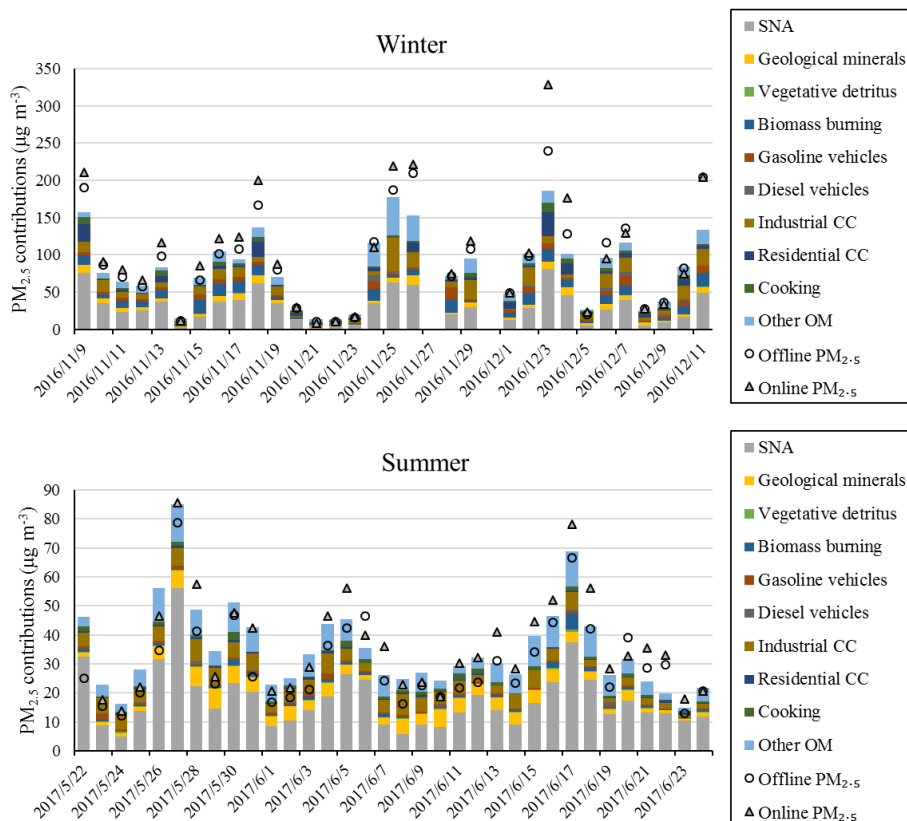
649 As shown in Table S4, PM<sub>2.5</sub> mass was well explained by those sources which  
650 accounted for 91.9±24.1% and 99.0±19.1% of online PM<sub>2.5</sub> in winter and summer,  
651 respectively. In the summer, the offline PM<sub>2.5</sub> is lower than online observations. Thus,  
652 the CMB-based source contributions are more than offline PM<sub>2.5</sub> mass (121.7±26.6%).  
653 On average, the source contributions in winter ranked as SNA (30.5 μg m<sup>-3</sup>, 34.1% of  
654 reconstructed PM<sub>2.5</sub> and hereafter), coal combustion (industrial & residential CC; 17.7  
655 μg m<sup>-3</sup>, 21.4%), Other OM (14.6 μg m<sup>-3</sup>, 14.8%), biomass burning (8.9 μg m<sup>-3</sup>, 11.0%),  
656 gasoline & diesel (5.6 μg m<sup>-3</sup>, 7.5%), geological minerals (5.3 μg m<sup>-3</sup>, 7.0%), cooking  
657 (3.1 μg m<sup>-3</sup>, 3.9%) and vegetative detritus (0.2 μg m<sup>-3</sup>, 0.3%); in summer these ranked  
658 as SNA (17.7 μg m<sup>-3</sup>, 48.5%), other OM (8.0 μg m<sup>-3</sup>, 18.3%), coal combustion (4.7 μg  
659 m<sup>-3</sup>, 14.6%), geological minerals (3.5 μg m<sup>-3</sup>, 10.4%), cooking (0.9 μg m<sup>-3</sup>, 2.8%),  
660 gasoline & diesel (0.8 μg m<sup>-3</sup>, 2.6%), biomass burning (0.8 μg m<sup>-3</sup>, 2.1%) and vegetative  
661 detritus (0.2 μg m<sup>-3</sup>, 0.7%).

662 Zheng et al. (2005) investigated the seasonal trends of PM<sub>2.5</sub> source contributions in  
663 Beijing during 2000 applying a CMB model. In winter (January), the contributions from  
664 coal combustion, biomass burning, diesel & gasoline, vegetative detritus to PM<sub>2.5</sub> were  
665 9.55 μg m<sup>-3</sup> (16% of PM<sub>2.5</sub> and hereafter), 5.8 μg m<sup>-3</sup> (9%), 3.85 μg m<sup>-3</sup>, 0.33 μg m<sup>-3</sup>,  
666 respectively. Contributions from gasoline, diesel, coal combustion and biomass burning  
667 were enhanced in Beijing during winter in 2016 compared to 2000, while the  
668 contribution from vegetative detritus basically remained similar. In summer (July) 2000,



669 coal combustion contributed 2% of  $PM_{2.5}$  ( $2.39 \mu g m^{-3}$ ), much less than that in summer  
670 2016 of this study. The contribution from diesel & gasoline ( $7.78 \mu g m^{-3}$ , Zheng et al.,  
671 2005) was approximately 10 times of that in 2016 ( $0.8 \mu g m^{-3}$ ). Similarly, contributions  
672 from vegetative detritus and biomass burning were small and insignificant.

673 Zhou et al. (2017) estimated that coal combustion contributions in winter and  
674 summer of Beijing-Tianjin-Hebei area in 2013 were  $15.9 \mu g m^{-3}$  and  $2.1 \mu g m^{-3}$ ,  
675 respectively, which are comparable with those in this study. These results are also  
676 comparable with the PMF-resolved coal and oil combustion in Beijing during winter  
677 ( $17.4 \mu g m^{-3}$ ) and summer ( $2.2 \mu g m^{-3}$ ) in 2010 (Yu et al., 2013). SNA contributed  $52.7$   
678 and  $26.4 \mu g m^{-3}$  of  $PM_{2.5}$  during winter (January) and summer (July), respectively (Yu  
679 et al., 2013), which are much higher than those in this study. It is noteworthy that a  
680 severe haze pollution event occurred during January 2013, which was characterized by  
681 high concentrations of sulfate and nitrate in several studies (Zhou et al., 2017; Han et  
682 al., 2016). The contribution from biomass burning in winter is consistent ( $8.5 \mu g m^{-3}$ )  
683 with this study ( $8.9 \mu g m^{-3}$ ), but higher in summer ( $2.6 \mu g m^{-3}$ ) ( $0.8 \mu g m^{-3}$ ). The  
684 cooking source contributed  $4.8$  and  $1.3 \mu g m^{-3}$  in  $PM_{2.5}$  during winter and summer 2013,  
685 respectively, which is also comparable with this study.



686  
687

**Figure 9.** Daily  $PM_{2.5}$  source contribution estimates from the CMB model

688



#### 689 4 Summary

690 Carbonaceous aerosols contributed approximately 59% and 41% of reconstructed PM<sub>2.5</sub>  
691 in winter and summer at the urban IAP site in Beijing. The OC and EC concentrations  
692 were comparable with more recent studies (Fan et al., 2020; Qi et al., 2018), but lower  
693 than those before 2013 (Yang et al., 2016; Dan et al., 2004), suggesting the  
694 effectiveness of air pollution control measures since 2013 (Vu et al., 2019; Zhang et al.,  
695 2019). CMB modelling showed that in the winter 2016, the top three primary  
696 contributors to PM<sub>2.5</sub>-OC were coal combustion (35%), biomass burning (17%), and  
697 traffic (12%); these were in the same order with that at the rural site during the same  
698 study period: coal combustion (29%), biomass burning (18%), and traffic (17%) (Wu  
699 et al., 2020). In the summer 2017, the top three primary contributors to PM<sub>2.5</sub>-OC were  
700 coal combustion (32%), cooking (11%), and traffic (6%); these were different to that at  
701 the rural site during the same study period: coal combustion (38%), biomass burning  
702 (11%), and traffic (7%) (Wu et al., 2020). The Other OC, which was well-correlated  
703 ( $R^2$ : 0.6~0.7; slope: 0.8~1.2) with the secondary OC (SOC) estimated based on the EC-  
704 tracer method, accounted for 25% and 44% of OC at urban site and 31% and 37% of  
705 OC at rural site during winter and summer, respectively. Although the annual average  
706 PM<sub>2.5</sub> levels in Beijing reduced from 88  $\mu\text{g m}^{-3}$  in year 2013 to 58  $\mu\text{g m}^{-3}$  in year 2017  
707 (Vu et al., 2019), and the deweathered concentration of PM<sub>1</sub> decreased by -38% in 2017  
708 comparing to 2007 (Zhang et al., 2020), our CMB modelling results indicate that the  
709 coal combustion and biomass burning still remained the dominant primary OC sources  
710 in 2016 winter and 2017 summer, with road traffic ranked as the third highest. Cooking  
711 was more significant than biomass burning at the urban site during summer. Compared  
712 to other CMB studies in Beijing, it revealed an increase of the contributions from coal  
713 combustion, biomass burning and traffic to PM<sub>2.5</sub> in winter 2016 compared to winter  
714 2000, while those in this study remained similar compared to winter 2013. Sulfate,  
715 nitrate and ammonium concentrations were significantly lower in this study compared  
716 to 2013 (Zheng et al., 2005; Zhou et al., 2017). It is however notable that there is a  
717 broad consistency in the findings of the CMB studies, whereas the more numerous  
718 studies which have used PMF come to rather diverse conclusions (Srivastava et al.,  
719 2020).

720

721 *Data availability.* The data in this article are available from the corresponding authors  
722 upon request.

723

724 *Author contributions.* JX did the CMB modelling and drafted the paper with the help  
725 of ZS, RMH and all co-authors. DL, TVV conducted the laboratory analysis of organics  
726 and inorganics, respectively. XW, YZ provided the CMB source profiles. YS provided  
727 the AMS-PMF data.

728

729 *Competing interests.* The authors have no conflict of interests.

730



731 *Acknowledgement.* This research was funded by the UK Natural Environment Research  
732 Council (NERC, NE/N007190/1; NE/R005281/1) and Royal Society Advanced  
733 Fellowship (grant no: NAF\R1\191220).

734

## 735 Reference

- 736 Aiken, A. C., DeCarlo, P. F., Kroll, J. H., Worsnop, D. R., Huffman, J. A., Docherty, K. S., Ulbrich, I. M.,  
737 Mohr, C., Kimmel, J. R., Sueper, D., Sun, Y., Zhang, Q., Trimborn, A., Northway, M., Ziemann, P. J.,  
738 Canagaratna, M. R., Onasch, T. B., Alfarra, M. R., Prevot, A. S. H., Dommen, J., Duplissy, J., Metzger,  
739 A., Baltensperger, U., and Jimenez, J. L.: O/C and OM/OC Ratios of Primary, Secondary, and Ambient  
740 Organic Aerosols with High-Resolution Time-of-Flight Aerosol Mass Spectrometry, *Environ. Sci.*  
741 *Technol.*, 42, 4478-4485, 10.1021/es703009q, 2008.
- 742 Aiken, A. C., Salcedo, D., Cubison, M. J., Huffman, J. A., DeCarlo, P. F., Ulbrich, I. M., Docherty, K. S.,  
743 Sueper, D., Kimmel, J. R., Worsnop, D. R., Trimborn, A., Northway, M., Stone, E. A., Schauer, J. J.,  
744 Volkamer, R. M., Fortner, E., de Foy, B., Wang, J., Laskin, A., Shutthanandan, V., Zheng, J., Zhang, R.,  
745 Gaffney, J., Marley, N. A., Paredes-Miranda, G., Arnott, W. P., Molina, L. T., Sosa, G., and Jimenez, J.  
746 L.: Mexico City aerosol analysis during MILAGRO using high resolution aerosol mass spectrometry at  
747 the urban supersite (T0) – Part 1: Fine particle composition and organic source apportionment, *Atmos.*  
748 *Chem. Phys.*, 9, 6633-6653, 10.5194/acp-9-6633-2009, 2009.
- 749 Bae, M.-S., Demerjian, K. L., and Schwab, J. J.: Seasonal estimation of organic mass to organic carbon  
750 in PM<sub>2.5</sub> at rural and urban locations in New York state, *Atmospheric Environment*, 40, 7467-7479,  
751 <https://doi.org/10.1016/j.atmosenv.2006.07.008>, 2006a.
- 752 Bae, M.-S., Schauer, J. J., and Turner, J. R.: Estimation of the Monthly Average Ratios of Organic Mass  
753 to Organic Carbon for Fine Particulate Matter at an Urban Site, *Aerosol Sci. Technol.*, 40, 1123-1139,  
754 10.1080/02786820601004085, 2006b.
- 755 Bhattarai, H., Saikawa, E., Wan, X., Zhu, H., Ram, K., Gao, S., Kang, S., Zhang, Q., Zhang, Y., Wu, G.,  
756 Wang, X., Kawamura, K., Fu, P., and Cong, Z.: Levoglucosan as a tracer of biomass burning: Recent  
757 progress and perspectives, *Atmos. Res.*, 220, 20-33, <https://doi.org/10.1016/j.atmosres.2019.01.004>,  
758 2019.
- 759 Cai, T., Zhang, Y., Fang, D., Shang, J., Zhang, Y., and Zhang, Y.: Chinese vehicle emissions characteristic  
760 testing with small sample size: Results and comparison, *Atmospheric Pollution Research*, 8, 154-163,  
761 <https://doi.org/10.1016/j.apr.2016.08.007>, 2017.
- 762 Castro, L. M., Pio, C. A., Harrison, R. M., and Smith, D. J. T.: Carbonaceous aerosol in urban and rural  
763 European atmospheres: estimation of secondary organic carbon concentrations, *Atmospheric*  
764 *Environment*, 33, 2771-2781, [https://doi.org/10.1016/S1352-2310\(98\)00331-8](https://doi.org/10.1016/S1352-2310(98)00331-8), 1999.
- 765 Chen, W.-N., Chen, Y.-C., Kuo, C.-Y., Chou, C.-H., Cheng, C.-H., Huang, C.-C., Chang, S.-Y., Roja  
766 Raman, M., Shang, W.-L., Chuang, T.-Y., and Liu, S.-C.: The real-time method of assessing the  
767 contribution of individual sources on visibility degradation in Taichung, *Science of The Total*  
768 *Environment*, 497-498, 219-228, <https://doi.org/10.1016/j.scitotenv.2014.07.120>, 2014.
- 769 Cheng, Y., Engling, G., He, K. B., Duan, F. K., Ma, Y. L., Du, Z. Y., Liu, J. M., Zheng, M., and Weber,  
770 R. J.: Biomass burning contribution to Beijing aerosol, *Atmospheric Chemistry And Physics*, 13, 7765-  
771 7781, 10.5194/acp-13-7765-2013, 2013.
- 772 Chow, J. C., Lowenthal, D. H., Chen, L. W. A., Wang, X. L., and Watson, J. G.: Mass reconstruction  
773 methods for PM<sub>2.5</sub>: a review, *Air Quality Atmosphere And Health*, 8, 243-263, 10.1007/s11869-015-  
774 0338-3, 2015.
- 775 Chuang, M.-T., Chen, Y.-C., Lee, C.-T., Cheng, C.-H., Tsai, Y.-J., Chang, S.-Y., and Su, Z.-S.:  
776 Apportionment of the sources of high fine particulate matter concentration events in a developing  
777 aerotropolis in Taoyuan, Taiwan, *Environmental Pollution*, 214, 273-281,  
778 <https://doi.org/10.1016/j.envpol.2016.04.045>, 2016.
- 779 Dan, M., Zhuang, G., Li, X., Tao, H., and Zhuang, Y.: The characteristics of carbonaceous species and  
780 their sources in PM<sub>2.5</sub> in Beijing, *Atmospheric Environment*, 38, 3443-3452,  
781 <https://doi.org/10.1016/j.atmosenv.2004.02.052>, 2004.
- 782 Dong, F.-m., Mo, Y.-z., Li, G.-x., Xu, M.-m., and Pan, X.-c.: [Association between ambient PM<sub>10</sub>/PM<sub>2.5</sub>  
783 levels and population mortality of circulatory diseases: a case-crossover study in Beijing], *Beijing Da*  
784 *Xue Xue Bao Yi Xue Ban*, 45, 398-404, 2013.
- 785 Elser, M., Huang, R. J., Wolf, R., Slowik, J. G., Wang, Q., Canonaco, F., Li, G., Bozzetti, C., Daellenbach,  
786 K. R., Huang, Y., Zhang, R., Li, Z., Cao, J., Baltensperger, U., El-Haddad, I., and Prévôt, A. S. H.: New





- 787 insights into PM<sub>2.5</sub> chemical composition and sources in two major cities in China during extreme haze  
788 events using aerosol mass spectrometry, *Atmos. Chem. Phys.*, 16, 3207–3225, 10.5194/acp-16-3207-  
789 2016, 2016.
- 790 Fan, Y., Liu, C. Q., Li, L., Ren, L., Ren, H., Zhang, Z., Li, Q., Wang, S., Hu, W., Deng, J., Wu, L., Zhong,  
791 S., Zhao, Y., Pavuluri, C. M., Li, X., Pan, X., Sun, Y., Wang, Z., Kawamura, K., Shi, Z., and Fu, P.: Large  
792 contributions of biogenic and anthropogenic sources to fine organic aerosols in Tianjin, North China,  
793 *Atmos. Chem. Phys.*, 20, 117–137, 10.5194/acp-20-117-2020, 2020.
- 794 Fountoukis, C., and Nenes, A.: ISORROPIA II: a computationally efficient thermodynamic equilibrium  
795 model for K<sup>+</sup>–Ca<sup>2+</sup>–Mg<sup>2+</sup>–NH<sub>4</sub><sup>+</sup>–Na<sup>+</sup>–SO<sub>4</sub><sup>2-</sup>–NO<sub>3</sub>–Cl–H<sub>2</sub>O aerosols, *Atmos. Chem. Phys.*, 7,  
796 4639–4659, 10.5194/acp-7-4639-2007, 2007.
- 797 Fu, P., Zhuang, G., Sun, Y., Wang, Q., Chen, J., Ren, L., Yang, F., Wang, Z., Pan, X., Li, X., and  
798 Kawamura, K.: Molecular markers of biomass burning, fungal spores and biogenic SOA in the  
799 Taklimakan desert aerosols, *Atmospheric Environment*, 130, 64–73, 10.1016/j.atmosenv.2015.10.087,  
800 2016.
- 801 Guo, S., Hu, M., Guo, Q., Zhang, X., Zheng, M., Zheng, J., Chang, C. C., Schauer, J. J., and Zhang, R.:  
802 Primary Sources and Secondary Formation of Organic Aerosols in Beijing, China, *Environ. Sci. Technol.*,  
803 46, 9846–9853, 10.1021/es2042564, 2012.
- 804 Guo, S., Hu, M., Guo, Q., Zhang, X., Schauer, J. J., and Zhang, R.: Quantitative evaluation of emission  
805 controls on primary and secondary organic aerosol sources during Beijing 2008 Olympics, *Atmos. Chem.*  
806 *Phys.*, 13, 8303–8314, 10.5194/acp-13-8303-2013, 2013.
- 807 Han, B., Zhang, R., Yang, W., Bai, Z., Ma, Z., and Zhang, W.: Heavy haze episodes in Beijing during  
808 January 2013: Inorganic ion chemistry and source analysis using highly time-resolved measurements  
809 from an urban site, *Science of The Total Environment*, 544, 319–329,  
810 <https://doi.org/10.1016/j.scitotenv.2015.10.053>, 2016.
- 811 He, K., Yang, F., Ma, Y., Zhang, Q., Yao, X., Chan, C. K., Cadle, S., Chan, T., and Mulawa, P.: The  
812 characteristics of PM<sub>2.5</sub> in Beijing, China, *Atmospheric Environment*, 35, 4959–4970,  
813 [https://doi.org/10.1016/S1352-2310\(01\)00301-6](https://doi.org/10.1016/S1352-2310(01)00301-6), 2001.
- 814 Hua, Y., Wang, S., Jiang, J., Zhou, W., Xu, Q., Li, X., Liu, B., Zhang, D., and Zheng, M.: Characteristics  
815 and sources of aerosol pollution at a polluted rural site southwest in Beijing, China, *Science of The Total*  
816 *Environment*, 626, 519–527, <https://doi.org/10.1016/j.scitotenv.2018.01.047>, 2018.
- 817 Huang, R.-J., Zhang, Y., Bozzetti, C., Ho, K.-F., Cao, J.-J., Han, Y., Daellenbach, K. R., Slowik, J. G.,  
818 Platt, S. M., Canonaco, F., Zotter, P., Wolf, R., Pieber, S. M., Bruns, E. A., Crippa, M., Ciarelli, G.,  
819 Piazzalunga, A., Schwikowski, M., Abbaszade, G., Schnelle-Kreis, J., Zimmermann, R., An, Z., Szidat,  
820 S., Baltensperger, U., Haddad, I. E., and Prévôt, A. S. H.: High secondary aerosol contribution to  
821 particulate pollution during haze events in China, *Nature*, 514, 218–222, 10.1038/nature13774, 2014.
- 822 Huang, X., Liu, Z., Liu, J., Hu, B., Wen, T., Tang, G., Zhang, J., Wu, F., Ji, D., Wang, L., and Wang, Y.:  
823 Chemical characterization and source identification of PM<sub>2.5</sub> at multiple sites in the Beijing–Tianjin–  
824 Hebei region, China, *Atmos. Chem. Phys.*, 17, 12941–12962, 10.5194/acp-17-12941-2017, 2017.
- 825 Huang, X. F., He, L. Y., Hu, M., Canagaratna, M. R., Sun, Y., Zhang, Q., Zhu, T., Xue, L., Zeng, L. W.,  
826 Liu, X. G., Zhang, Y. H., Jayne, J. T., Ng, N. L., and Worsnop, D. R.: Highly time-resolved chemical  
827 characterization of atmospheric submicron particles during 2008 Beijing Olympic Games using an  
828 Aerodyne High-Resolution Aerosol Mass Spectrometer, *Atmos. Chem. Phys.*, 10, 8933–8945,  
829 10.5194/acp-10-8933-2010, 2010.
- 830 Kang, M., Ren, L., Ren, H., Zhao, Y., Kawamura, K., Zhang, H., Wei, L., Sun, Y., Wang, Z., and Fu, P.:  
831 Primary biogenic and anthropogenic sources of organic aerosols in Beijing, China: Insights from  
832 saccharides and n-alkanes, *Environmental Pollution*, 243, 1579–1587,  
833 <https://doi.org/10.1016/j.envpol.2018.09.118>, 2018.
- 834 Li, L., Ren, L., Ren, H., Yue, S., Xie, Q., Zhao, W., Kang, M., Li, J., Wang, Z., Sun, Y., and Fu, P.:  
835 Molecular Characterization and Seasonal Variation in Primary and Secondary Organic Aerosols in  
836 Beijing, China, 2018.
- 837 Li, P., Xin, J., Wang, Y., Wang, S., Li, G., Pan, X., Liu, Z., and Wang, L.: The acute effects of fine particles  
838 on respiratory mortality and morbidity in Beijing, 2004–2009, *Environ. Sci. Pollut. Res.*, 20, 6433–6444,  
839 10.1007/s11356-013-1688-8, 2013.
- 840 Li, X., Nie, T., Qi, J., Zhou, Z., and Sun, X. S.: [Regional Source Apportionment of PM<sub>2.5</sub> in Beijing in  
841 January 2013], *Huan jing ke xue= Huanjing kexue*, 36, 1148–1153, 2015.
- 842 Liu, B., Wu, J., Zhang, J., Wang, L., Yang, J., Liang, D., Dai, Q., Bi, X., Feng, Y., Zhang, Y., and Zhang,  
843 Q.: Characterization and source apportionment of PM<sub>2.5</sub> based on error estimation from EPA PMF 5.0  
844 model at a medium city in China, *Environmental Pollution*, 222, 10–22,  
845 <https://doi.org/10.1016/j.envpol.2017.01.005>, 2017.
- 846 Liu, Q., Baumgartner, J., Zhang, Y., and Schauer, J. J.: Source apportionment of Beijing air pollution



- 847 during a severe winter haze event and associated pro-inflammatory responses in lung epithelial cells,  
848 Atmospheric Environment, 126, 28-35, <https://doi.org/10.1016/j.atmosenv.2015.11.031>, 2016.
- 849 Pant, P., Shukla, A., Kohl, S. D., Chow, J. C., Watson, J. G., and Harrison, R. M.: Characterization of  
850 ambient PM<sub>2.5</sub> at a pollution hotspot in New Delhi, India and inference of sources, Atmospheric  
851 Environment, 109, 178-189, <https://doi.org/10.1016/j.atmosenv.2015.02.074>, 2015.
- 852 Paraskevopoulou, D., Liakakou, E., Gerasopoulos, E., Theodosi, C., and Mihalopoulos, N.: Long-term  
853 characterization of organic and elemental carbon in the PM<sub>>2.5</sub> fraction: the case of Athens,  
854 Greece, Atmos. Chem. Phys., 14, 13313-13325, [10.5194/acp-14-13313-2014](https://doi.org/10.5194/acp-14-13313-2014), 2014.
- 855 Pio, C., and Harrison, R.: Vapour pressure of ammonium chloride aerosol: Effect of temperature and  
856 humidity, Atmospheric Environment (1967), 21, 2711-2715, [10.1016/0004-6981\(87\)90203-4](https://doi.org/10.1016/0004-6981(87)90203-4), 1987.
- 857 Pio, C., Cerqueira, M., Harrison, R. M., Nunes, T., Mirante, F., Alves, C., Oliveira, C., Sanchez de la  
858 Campa, A., Artíñano, B., and Matos, M.: OC/EC ratio observations in Europe: Re-thinking the approach  
859 for apportionment between primary and secondary organic carbon, Atmospheric Environment, 45, 6121-  
860 6132, <https://doi.org/10.1016/j.atmosenv.2011.08.045>, 2011.
- 861 Qi, M., Jiang, L., Liu, Y., Xiong, Q., Sun, C., Li, X., Zhao, W., and Yang, X.: Analysis of the  
862 Characteristics and Sources of Carbonaceous Aerosols in PM<sub>2.5</sub> in the Beijing, Tianjin, and Langfang  
863 Region, China, Int J Environ Res Public Health, 15, 1483, [10.3390/ijerph15071483](https://doi.org/10.3390/ijerph15071483), 2018.
- 864 Rogge, W. F., Hildemann, L. M., Mazurek, M. A., Cass, G. R., and Simoneit, B. R. T.: Sources of fine  
865 organic aerosol. 4. Particulate abrasion products from leaf surfaces of urban plants, Environ. Sci. Technol.,  
866 27, 2700-2711, [10.1021/es00049a008](https://doi.org/10.1021/es00049a008), 1993.
- 867 Shi, Z., Vu, T., Kotthaus, S., Harrison, R. M., Grimmond, S., Yue, S., Zhu, T., Lee, J., Han, Y., Demuzere,  
868 M., Dunmore, R. E., Ren, L., Liu, D., Wang, Y., Wild, O., Allan, J., Acton, W. J., Barlow, J., Barratt, B.,  
869 Beddows, D., Bloss, W. J., Calzolari, G., Carruthers, D., Carslaw, D. C., Chan, Q., Chatzidiakou, L., Chen,  
870 Y., Crilley, L., Coe, H., Dai, T., Doherty, R., Duan, F., Fu, P., Ge, B., Ge, M., Guan, D., Hamilton, J. F.,  
871 He, K., Heal, M., Heard, D., Hewitt, C. N., Holloway, M., Hu, M., Ji, D., Jiang, X., Jones, R., Kalberer,  
872 M., Kelly, F. J., Kramer, L., Langford, B., Lin, C., Lewis, A. C., Li, J., Li, W., Liu, H., Liu, J., Loh, M.,  
873 Lu, K., Lucarelli, F., Mann, G., McFiggans, G., Miller, M. R., Mills, G., Monk, P., Nemitz, E., O'Connor,  
874 F., Ouyang, B., Palmer, P. I., Percival, C., Popoola, O., Reeves, C., Rickard, A. R., Shao, L., Shi, G.,  
875 Spracklen, D., Stevenson, D., Sun, Y., Sun, Z., Tao, S., Tong, S., Wang, Q., Wang, W., Wang, X., Wang,  
876 X., Wang, Z., Wei, L., Whalley, L., Wu, X., Wu, Z., Xie, P., Yang, F., Zhang, Q., Zhang, Y., Zhang, Y.,  
877 and Zheng, M.: Introduction to the special issue "In-depth study of air pollution sources and processes  
878 within Beijing and its surrounding region (APHH-Beijing)", Atmos. Chem. Phys., 19, 7519-7546,  
879 [10.5194/acp-19-7519-2019](https://doi.org/10.5194/acp-19-7519-2019), 2019.
- 880 Song, Y., Xie, S., Zhang, Y., Zeng, L., Salmon, L. G., and Zheng, M.: Source apportionment of PM<sub>2.5</sub> in  
881 Beijing using principal component analysis/absolute principal component scores and UNMIX, Science  
882 of The Total Environment, 372, 278-286, <https://doi.org/10.1016/j.scitotenv.2006.08.041>, 2006a.
- 883 Song, Y., Zhang, Y., Xie, S., Zeng, L., Zheng, M., Salmon, L. G., Shao, M., and Slanina, S.: Source  
884 apportionment of PM<sub>2.5</sub> in Beijing by positive matrix factorization, Atmospheric Environment, 40,  
885 1526-1537, <https://doi.org/10.1016/j.atmosenv.2005.10.039>, 2006b.
- 886 Song, Y., Tang, X., Xie, S., Zhang, Y., Wei, Y., Zhang, M., Zeng, L., and Lu, S.: Source apportionment  
887 of PM<sub>2.5</sub> in Beijing in 2004, Journal of Hazardous Materials, 146, 124-130,  
888 <https://doi.org/10.1016/j.jhazmat.2006.11.058>, 2007.
- 889 Srivastava, D., Favez, O., Petit, J. E., Zhang, Y., Sofowote, U. M., Hopke, P. K., Bonnaire, N., Perraudin,  
890 E., Gros, V., Villenave, E., and Albinet, A.: Speciation of organic fractions does matter for aerosol source  
891 apportionment. Part 3: Combining off-line and on-line measurements, Science of The Total Environment,  
892 690, 944-955, <https://doi.org/10.1016/j.scitotenv.2019.06.378>, 2019.
- 893 Srivastava, D., Xu, J., Liu, D., Vu, T. V., Shi, Z., and Harrison, R. M.: Insight into PM<sub>2.5</sub> sources by  
894 applying Positive Matrix factorization (PMF) at urban and rural sites of Beijing, Atmospheric Chemistry  
895 and Physics (under review), 2020.
- 896 Sun, Y., Du, W., Fu, P., Wang, Q., Li, J., Ge, X., Zhang, Q., Zhu, C., Ren, L., Xu, W., Zhao, J., Han, T.,  
897 Worsnop, D. R., and Wang, Z.: Primary and secondary aerosols in Beijing in winter: sources, variations  
898 and processes, Atmos. Chem. Phys., 16, 8309-8329, [10.5194/acp-16-8309-2016](https://doi.org/10.5194/acp-16-8309-2016), 2016.
- 899 Sun, Y., He, Y., Kuang, Y., Xu, W., Song, S., Ma, N., Tao, J., Cheng, P., Wu, C., Su, H., Cheng, Y., Xie,  
900 C., Chen, C., Lei, L., Qiu, Y., Fu, P., Croteau, P., and Worsnop, D. R.: Chemical Differences between  
901 PM<sub>1</sub> and PM<sub>2.5</sub> in Highly Polluted Environment and Implications in Air Pollution Studies, Geophysical  
902 Research Letters, n/a, [e2019GL086288](https://doi.org/10.1029/2019gl086288), [10.1029/2019gl086288](https://doi.org/10.1029/2019gl086288), 2020.
- 903 Turpin, B. J., and Huntzicker, J. J.: Identification of secondary organic aerosol episodes and quantitation  
904 of primary and secondary organic aerosol concentrations during SCAQS, Atmospheric Environment, 29,  
905 3527-3544, [https://doi.org/10.1016/1352-2310\(94\)00276-Q](https://doi.org/10.1016/1352-2310(94)00276-Q), 1995.
- 906 Ulbrich, I. M., Canagaratna, M. R., Zhang, Q., Worsnop, D. R., and Jimenez, J. L.: Interpretation of



- 907 organic components from Positive Matrix Factorization of aerosol mass spectrometric data, *Atmos.*  
908 *Chem. Phys.*, 9, 2891-2918, 10.5194/acp-9-2891-2009, 2009.
- 909 Vu, T. V., Shi, Z. B., Cheng, J., Zhang, Q., He, K. B., Wang, S. X., and Harrison, R. M.: Assessing the  
910 impact of clean air action on air quality trends in Beijing using a machine learning technique,  
911 *Atmospheric Chemistry And Physics*, 19, 11303-11314, 10.5194/acp-19-11303-2019, 2019.
- 912 Wang, Q., Shao, M., Zhang, Y., Wei, Y., Hu, M., and Guo, S.: Source apportionment of fine organic  
913 aerosols in Beijing, *Atmos. Chem. Phys.*, 9, 8573-8585, 10.5194/acp-9-8573-2009, 2009.
- 914 Wu, X., Chen, C., Vu, T. V., Liu, D., Baldo, C., Shen, X., Zhang, Q., Cen, K., Zheng, M., He, K., Shi, Z.,  
915 and Harrison, R. M.: Source Apportionment of Fine Organic Carbon (OC) Using Receptor Modelling at  
916 a Rural Site of Beijing: Insight into Seasonal and Diurnal Variation of Source Contributions,  
917 *Environmental Pollution* (under review), 2020.
- 918 Xu, J., Jia, C., He, J., Xu, H., Tang, Y.-T., Ji, D., Yu, H., Xiao, H., and Wang, C.: Biomass burning and  
919 fungal spores as sources of fine aerosols in Yangtze River Delta, China – Using multiple organic tracers  
920 to understand variability, correlations and origins, *Environmental Pollution*, 251, 155-165,  
921 <https://doi.org/10.1016/j.envpol.2019.04.090>, 2019a.
- 922 Xu, J., Song, S., Harrison, R. M., Song, C., Wei, L., Zhang, Q., Sun, Y., Lei, L., Zhang, C., Yao, X., Chen,  
923 D., Li, W., Wu, M., Tian, H., Luo, L., Tong, S., Li, W., Wang, J., Shi, G., Huangfu, Y., Tian, Y., Ge, B.,  
924 Su, S., Peng, C., Chen, Y., Yang, F., Mihajlidi-Zelić, A., Đorđević, D., Swift, S. J., Andrews, I., Hamilton,  
925 J. F., Sun, Y., Kramawijaya, A., Han, J., Saksakulkrai, S., Baldo, C., Hou, S., Zheng, F., Daellenbach, K.  
926 R., Yan, C., Liu, Y., Kulmala, M., Fu, P., and Shi, Z.: An inter-laboratory comparison of aerosol in organic  
927 ion measurements by Ion Chromatography: implications for aerosol pH estimate, *Atmos. Meas. Tech.*  
928 *Discuss.*, 2020, 1-36, 10.5194/amt-2020-156, 2020.
- 929 Xu, M., Yu, D., Yao, H., Liu, X., and Qiao, Y.: Coal combustion-generated aerosols: Formation and  
930 properties, *Proceedings of the Combustion Institute*, 33, 1681-1697,  
931 <https://doi.org/10.1016/j.proci.2010.09.014>, 2011.
- 932 Xu, W., Sun, Y., Wang, Q., Zhao, J., Wang, J., Ge, X., Xie, C., Zhou, W., Du, W., Li, J., Fu, P., Wang, Z.,  
933 Worsnop, D. R., and Coe, H.: Changes in Aerosol Chemistry From 2014 to 2016 in Winter in Beijing:  
934 Insights From High-Resolution Aerosol Mass Spectrometry, *Journal of Geophysical Research:*  
935 *Atmospheres*, 124, 1132-1147, 10.1029/2018jd029245, 2019b.
- 936 Xu, X., Zhang, H., Chen, J., Li, Q., Wang, X., Wang, W., Zhang, Q., Xue, L., Ding, A., and Mellouki, A.:  
937 Six sources mainly contributing to the haze episodes and health risk assessment of PM<sub>2.5</sub> at Beijing  
938 suburb in winter 2016, *Ecotoxicology and Environmental Safety*, 166, 146-156,  
939 <https://doi.org/10.1016/j.ecoenv.2018.09.069>, 2018.
- 940 Yang, F., Kawamura, K., Chen, J., Ho, K., Lee, S., Gao, Y., Cui, L., Wang, T., and Fu, P.: Anthropogenic  
941 and biogenic organic compounds in summertime fine aerosols (PM<sub>2.5</sub>) in Beijing, China, *Atmospheric*  
942 *Environment*, 124, 166-175, <https://doi.org/10.1016/j.atmosenv.2015.08.095>, 2016.
- 943 Yu, L., and Wang, G.: Characterization and Source Apportionment of PM<sub>2.5</sub> in an Urban Environment  
944 in Beijing, *Aerosol Air Qual. Res.*, 13, 10.4209/aaqr.2012.07.0192, 2013.
- 945 Yu, L. D., Wang, G. F., Zhang, R. J., Zhang, L. M., Song, Y., Wu, B. B., Li, X. F., An, K., and Chu, J. H.:  
946 Characterization and Source Apportionment of PM<sub>2.5</sub> in an Urban Environment in Beijing, *Aerosol Air*  
947 *Qual. Res.*, 13, 574-583, 10.4209/aaqr.2012.07.0192, 2013.
- 948 Yu, S., Liu, W., Xu, Y., Yi, K., Zhou, M., Tao, S., and Liu, W.: Characteristics and oxidative potential of  
949 atmospheric PM<sub>2.5</sub> in Beijing: Source apportionment and seasonal variation, *Science of The Total*  
950 *Environment*, 650, 277-287, <https://doi.org/10.1016/j.scitotenv.2018.09.021>, 2019.
- 951 Zhang, Q., Worsnop, D. R., Canagaratna, M. R., and Jimenez, J. L.: Hydrocarbon-like and oxygenated  
952 organic aerosols in Pittsburgh: insights into sources and processes of organic aerosols, *Atmospheric*  
953 *Chemistry And Physics*, 5, 3289-3311, 10.5194/acp-5-3289-2005, 2005.
- 954 Zhang, Q., Zheng, Y., Tong, D., Shao, M., Wang, S., Zhang, Y., Xu, X., Wang, J., He, H., Liu, W., Ding,  
955 Y., Lei, Y., Li, J., Wang, Z., Zhang, X., Wang, Y., Cheng, J., Liu, Y., Shi, Q., Yan, L., Geng, G., Hong, C.,  
956 Li, M., Liu, F., Zheng, B., Cao, J., Ding, A., Gao, J., Fu, Q., Huo, J., Liu, B., Liu, Z., Yang, F., He, K.,  
957 and Hao, J.: Drivers of improved PM<sub>2.5</sub> air quality in China from 2013 to 2017,  
958 *Proceedings of the National Academy of Sciences*, 116, 24463-24469, 10.1073/pnas.1907956116, 2019.
- 959 Zhang, R., Jing, J., Tao, J., Hsu, S. C., Wang, G., Cao, J., Lee, C. S. L., Zhu, L., Chen, Z., Zhao, Y., and  
960 Shen, Z.: Chemical characterization and source apportionment of PM<sub>2.5</sub> in Beijing:  
961 seasonal perspective, *Atmos. Chem. Phys.*, 13, 7053-7074, 10.5194/acp-13-7053-2013, 2013.
- 962 Zhang, X. Y., Zhuang, G. S., Guo, J. H., Yin, K. D., and Zhang, P.: Characterization of aerosol over the  
963 Northern South China Sea during two cruises in 2003, *Atmospheric Environment*, 41, 7821-7836,  
964 10.1016/j.atmosenv.2007.06.031, 2007a.
- 965 Zhang, Y.-x., Shao, M., Zhang, Y.-h., Zeng, L.-m., He, L.-y., Zhu, B., Wei, Y.-j., and Zhu, X.-l.: Source  
966 profiles of particulate organic matters emitted from cereal straw burnings, *Journal of Environmental*



- 967 Sciences, 19, 167-175, [https://doi.org/10.1016/S1001-0742\(07\)60027-8](https://doi.org/10.1016/S1001-0742(07)60027-8), 2007b.
- 968 Zhang, Y., Schauer, J. J., Zhang, Y., Zeng, L., Wei, Y., Liu, Y., and Shao, M.: Characteristics of Particulate  
969 Carbon Emissions from Real-World Chinese Coal Combustion, *Environ. Sci. Technol.*, 42, 5068-5073,  
970 10.1021/es7022576, 2008.
- 971 Zhang, Y., Vu, T. V., Sun, J., He, J., Shen, X., Lin, W., Zhang, X., Zhong, J., Gao, W., Wang, Y., Fu, T.  
972 M., Ma, Y., Li, W., and Shi, Z.: Significant Changes in Chemistry of Fine Particles in Wintertime Beijing  
973 from 2007 to 2017: Impact of Clean Air Actions, *Environ. Sci. Technol.*, 54, 1344-1352,  
974 10.1021/acs.est.9b04678, 2020.
- 975 Zhao, B., Zheng, H., Wang, S., Smith, K. R., Lu, X., Aunan, K., Gu, Y., Wang, Y., Ding, D., Xing, J., Fu,  
976 X., Yang, X., Liou, K.-N., and Hao, J.: Change in household fuels dominates the decrease in  
977 PM<sub>2.5</sub> exposure and premature mortality in China in 2005–2015, *Proceedings of the*  
978 *National Academy of Sciences*, 115, 12401-12406, 10.1073/pnas.1812955115, 2018.
- 979 Zhao, X., Hu, Q., Wang, X., Ding, X., He, Q., Zhang, Z., Shen, R., Lü, S., Liu, T., Fu, X., and Chen, L.:  
980 Composition profiles of organic aerosols from Chinese residential cooking: case study in urban  
981 Guangzhou, south China, *Journal of Atmospheric Chemistry*, 72, 1-18, 10.1007/s10874-015-9298-0,  
982 2015.
- 983 Zhao, Y., Hu, M., Slanina, S., and Zhang, Y.: Chemical Compositions of Fine Particulate Organic Matter  
984 Emitted from Chinese Cooking, *Environ. Sci. Technol.*, 41, 99-105, 10.1021/es0614518, 2007.
- 985 Zheng, B., Tong, D., Li, M., Liu, F., Hong, C., Geng, G., Li, H., Li, X., Peng, L., Qi, J., Yan, L., Zhang,  
986 Y., Zhao, H., Zheng, Y., He, K., and Zhang, Q.: Trends in China's anthropogenic emissions since 2010 as  
987 the consequence of clean air actions, *Atmos. Chem. Phys.*, 18, 14095-14111, 10.5194/acp-18-14095-  
988 2018, 2018.
- 989 Zheng, M., Salmon, L. G., Schauer, J. J., Zeng, L., Kiang, C. S., Zhang, Y., and Cass, G. R.: Seasonal  
990 trends in PM<sub>2.5</sub> source contributions in Beijing, China, *Atmospheric Environment*, 39, 3967-3976,  
991 <https://doi.org/10.1016/j.atmosenv.2005.03.036>, 2005.
- 992 Zhou, J., Xiong, Y., Xing, Z., Deng, J., and Du, K.: Characterizing and sourcing ambient PM<sub>2.5</sub> over key  
993 emission regions in China II: Organic molecular markers and CMB modeling, *Atmospheric Environment*,  
994 163, 57-64, <https://doi.org/10.1016/j.atmosenv.2017.05.033>, 2017.
- 995 Zhou, W., Wang, Q., Zhao, X., Xu, W., Chen, C., Du, W., Zhao, J., Canonaco, F., Prévôt, A. S. H., Fu, P.,  
996 Wang, Z., Worsnop, D. R., and Sun, Y.: Characterization and source apportionment of organic aerosol at  
997 260 m on a meteorological tower in Beijing, China, *Atmos. Chem. Phys.*, 18, 3951-3968,  
998 10.5194/acp-18-3951-2018, 2018.
- 999